AGE-SPECIFIC AND SPECIES-SPECIFIC TREE RESPONSE TO SEASONAL DROUGHT IN TROPICAL DRY FORESTS

By

Emily A. Santos

A Thesis Presented to

The Faculty of Humboldt State University

In Partial Fulfillment of the Requirements for the Degree

Master of Science in Environmental Systems: Geology

Committee Membership

Dr. Jasper Oshun, Committee Chair

Dr. Lucy Kerhoulas, Committee Member

Dr. Andrew Stubblefield, Committee Member

Dr. Brandon Browne, Committee Member

Dr. Margaret Lang, Program Graduate Coordinator

July 2020

ABSTRACT

AGE-SPECIFIC AND SPECIES-SPECIFIC TREE RESPONSE TO SEASONAL DROUGHT IN TROPICAL DRY FORESTS

Emily A. Santos

Millions of people live in or depend on ecoregions dominated by Tropical Dry Forests (TDFs), but due to their high accessibility, convenient topography and mild climate conditions their distribution is fragmented with less than 10% of their original extent remaining in many countries. Despite the vast ecosystem services provided by TDFs, including vital water resources in water limited environments, ecohydrological research in this biome has been limited to a small number of short-term investigations. Similar to worldwide trends, the TDF surrounding Bahía de Caráquez (Bahía), Ecuador, has been severely deforested over the past 400 years. The land use history in Bahía, which has resulted in TDFs of different age and disturbance, provides a valuable setting to study the relationship between forest age and TDF hydrology. This thesis, conducted in the Cordillera del Balsamo (a local landowner-managed bio-corridor of protected TDF) presents the results of one year of frequent monitoring to explore subsurface moisture dynamics and species-specific water use strategies across TDFs of different ages. We 1) captured snapshots of changes in subsurface water content with direct measurements of shallow subsurface moisture and measurements of predawn and midday plant water potential, and 2) identified seasonal patterns in tree water use by analyzing the stable

isotope composition of bulk soil and bulk saprolite moisture, rainwater, groundwater, and tree xylem water. Our results over the transition from wet season to dry season in 2018 show that moisture is held at greater tensions, and thus is likely less available to trees in disturbed TDFs (<100 years old) than in old growth TDFs. We found there was insufficient seasonally dynamic moisture storage in the top meter to sustain expected rates of TDF transpiration, and that trees relied on moisture stored in weathered bedrock. The results of our stable isotope monitoring uncovered age-specific differences in tree water source and confirmed our hypothesis that younger trees growing in disturbed, secondary forests (<100 years old) must rely on deeper water sources below the soil to maintain physiological function into the dry period. In the secondary forest, the combined results of subsurface moisture data, predawn and midday water potentials, and stable isotopes allowed us to interpret three distinct water use strategies in three native TDF species: (1) the deeply rooted *Ceiba trichistandra* accesses deep sources of water held at relatively low water potentials through the dry season; (2) *Sideroxylon celastrinum* accesses shallow water in the early dry season and deep water in the late dry season via a dimorphic rooting system; and (3) *Tabebuia chrysantha* achieves the lowest midday water potentials and accesses soil and saprolite moisture late into the dry season, but also accesses deeper sources of moisture either directly or indirectly via hydraulic lift of neighboring trees. The results presented here may inform site specific or regional studies that quantify the effects of land use history on transpiration, subsurface water storage, groundwater recharge, and forest water yield in order to guide forest regeneration while achieving water security for human communities.

ACKNOWLEDGEMENTS

I first would like to thank my committee members, Dr. Jasper Oshun, Dr. Lucy Kerhoulas, Dr. Andrew Stubblefield and Dr. Brandon Browne for their valuable input and feedback. I also thank Dr. Oshun for contributing to presentations for both the American Geophysical Union and The Association for Tropical Biology and Conservation.

Thank you to those whose generosity made this thesis possible financially: The Consortium of Universities for the Advancement of Hydrologic Science, Inc. (CUAHSI) for the 2019 Instrumentation Discovery Travel Grant and the 2019 Graduate Student Travel Grant; Humboldt State University Department of Geology for the 2019 Geology Field Work Summer Assistance Award and the 2018 Geology Opportunities Fund Award; Andrea and Don Tuttle for the 2019 Tuttle Climate Conference Scholarship; The California State University Program for Education & Research in Biotechnology (CSUPERB) for the 2018 Graduate Student Travel Grant; Humboldt State University and Dr. Bud Burke for the 2017-2018 Bud Burke Scholarship.

Infinite thanks to my Corredores de Conservación de Biorregiones collaborators, Ramón Cedeno Loor and Blas Loor, whom without this study would not be possible. Thank you as well to my summer 2018 Field assistants: Katherine Castillo, Gretchen Johnson, and Miyako Namba. A very special thanks to Haley Sellers and Amanda Donaldson.

In closing I would like to acknowledge the efforts of Gustavo Torres, the Regeneration Field Institute, and Walking Palms Global Health in helping to provide equipment, housing, and helping hands during fieldwork, as well as the hospitality of the University of California Berkeley Center for Stable Isotope Biogeochemistry, particularly Dr. Stefania Mambelli and Dr. Wenbo Yang.

TABLE OF CONTENTS

LIST OF TABLES

LIST OF FIGURES

INTRODUCTION

Tropical Dry Forests (TDFs) are found between the latitudes of 23.5° North and South in areas where annual rainfall ranges from 250–2000 mm with a marked dry season of at least five through six months (Murphy & Lugo, 1986; Bullock et al., 1995; Miles et al., 2006). This results in dramatic changes in the appearance of a TDF between the wet and dry season as shown in pictures of the TDF of coastal Ecuador (Figure 1). The amount and seasonality of rainfall strongly influence eco-hydrological processes as well as tree phenology, structure, and drought coping strategies (Borchert, 1994; Schwinning & Ehleringer, 2001; Borchert et al., 2004; Sánchez-Azofeifa et al., 2005; Pennington et al., 2009). As a result, TDFs house high biodiversity, as species develop specific adaptations to exist in a water-limited environment (Kennard, 2002; Pennington et al., 2009; Horstman, 2017). TDFs are dominated by at least 50% drought-tolerant deciduous trees, lianas, shrubs, herbs, graminoids, agave, cacti and bromeliads. TDFs provide habitat for migratory birds, native butterflies, moths, bees, wasps and ants, as well as endangered mammals and reptiles (such as the Asian elephant, the world's most endangered tortoise Angonoka, the rare Timor Python, and the world's largest living lizard Komodo Dragon) (Banda et al., 2016). Many of these species are endemic, which leads to a biome that is often as rich in genetic and biological diversity as tropical rain forests (Janzen, 1988; Espinosa, Carlos I., et al., 2011; Wright et al., 2018).

Figure 1. More than any other factor, the combination of perennially high solar radiation and the absence of precipitation during a prolonged portion of the year is what results in Tropical Dry Forest, an ecosystem type characterized by plants and animals possessing specific adaptations to survive the dry season (Murphy & Lugo, 1986). Here we show contrasting images of the same TDF near Bahía de Caraquez, Ecuador in the middle of the wet season (March) and the end of the dry season (December).

While TDFs thrive in some parts of the world, they have had a historically high rate of resource exploitation and are among the least protected and most vulnerable ecosystems on Earth (Janzen, 1988; Hoekstra et al., 2005; Miles et al., 2006; Portillo-Quintero et al., 2010; Hansen, 2010; Gillespie et al., 2012). TDFs are located on relatively flat terrains, experience distinct wet and dry seasons, host medium biomass and structural complexity and a high number of above- and below ground freshwater sources. These factors make TDFs ideal areas to deforest for short-cycle crop agriculture and livestock farming (Miles et al., 2006; Portillo-Quintero et al., 2010; Portillo-Quintero et al., 2015). Particularly in the Americas, this type of land cover change was generally

driven by governmental policies based on the perception that the 'best' use for TDFs was to harvest wood and clear cut the land to make from for intensive agricultural production (Castillo et al., 2005; Quesada et al., 2009). TDFs have the third highest deforestation rate globally (Stan & Sanchez-Azofeifa, 2019) and their distribution is fragmented with less than 10% of their original extent remaining in many countries (Banda et al., 2016). Although TDFs are found in Africa, Central Asia, India, and Australia (Figure 2) (Quesada et al., 2009; Buzzard et al., 2016; Stan & Sanchez-Azofeifa, 2019), between 50% and 75% of the remaining TDF is located in Central and South America (Miles et al., 2006; Portillo-Quintero et al., 2010; Sanchez-Azofeifa et al., 2013).

.

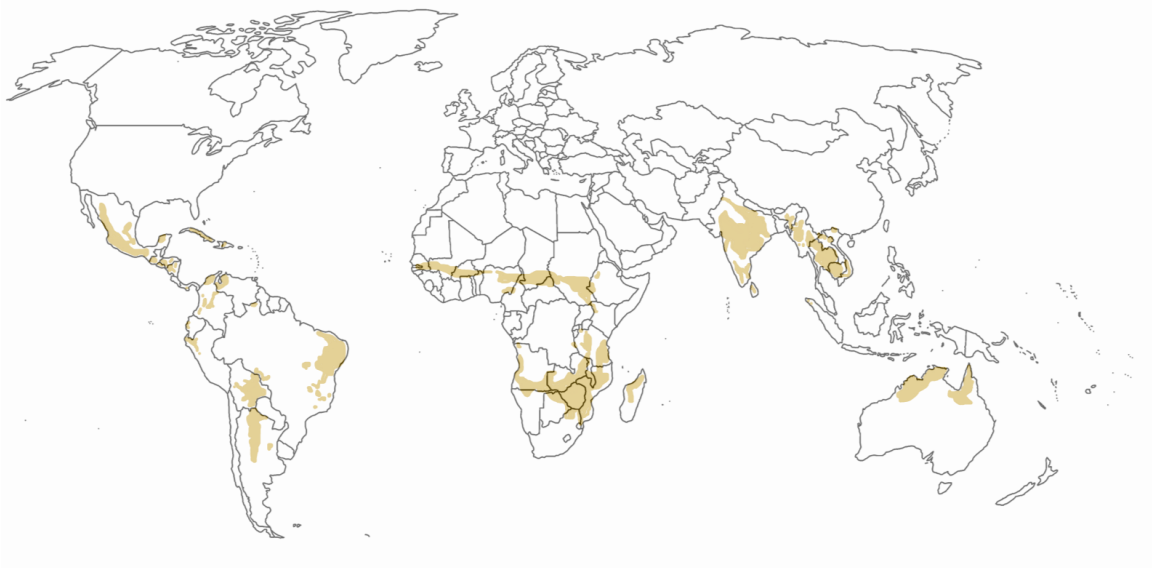

Figure 2. The global extent of Tropical Dry Forests as a modified reproduction based on 2010 global ecological zones for Food and Agriculture Organization (FAO) forest reporting. Approximately 90 million people live in or depend on ecoregions dominated

by dry forests, but due to their high accessibility, convenient topography and mild climate conditions their distribution is fragmented (Banda et al. 2016). Of the current TDFs worldwide, 97% of them are deemed at risk for proximate and indirect loss, jeopardizing the ecosystem services they provide (Miles et al. 2006; Cueva Ortiz et al., 2019).

Similar to global trends, coastal Ecuador followed the patterns of TDF deforestation for agriculture and pasture abandonment. All but 2% of coastal Ecuador's TDFs have been removed, and primary TDF, greater than 400 years old, is found only in the most inaccessible areas. From 2000-2008 alone, 6.75 km^2 of TDF (an area three times the size of San Francisco) was converted to pasture, annual crop, and urban area to accommodate growing populations (*Plan de Desarrollo y Ordenamiento Territorial*). Because of these tremendous, and exponential rates of loss organisms that once were common in these forests now face extinction for lack of habitat (Figure 3). Although TDFs are not adequately represented in the current national protected area system, Ecuadorian law allows landowners to declare private land as protected (Horstman, 2017). Nevertheless, few intact stands of TDF remain in the region of Bahía de Caráquez (Bahía), Ecuador. Of the remaining forest patches, some are selectively logged while others are well preserved partially due to landowner decisions.

Figure 3. TDFs are dominated by: **a.** epiphites (*Tillandsia usneoides*), **b.** orchids, **c.** bromeliads (*Tillandsia* sp.), **d.** cacti (*Hylocereus lemairei*), drought-tolerant deciduous trees **e.** (*Erythrina velutina*), **f.** (*Tabebuia chrysantha*), **g.** (*Ceiba trichistandra*), and provide habitat for **h.** birds (*Pheucticus chrysogaster*), **i.** arachnids (*Pamphobeteus sp.*), **j.** butterflies, and **k.** amphibians.

Despite the wealth of opportunities offered by these tremendously species-rich ecosystems, ecohydrological research has been limited to a small number of short-term investigations, in sharp contrast with the large body of literature on the ecohydrology of temperate and tropical humid forest watersheds (Sánchez-Azofeifa et al., 2005; Quesada et al., 2009; Portillo-Quintero et al., 2010; Farrick & Branfireun, 2014; Calvo-Rodriquez, 2017; Wright et al., 2018; Stan & Sanchez-Azofeifa, 2019). Studies examining forests and water in South America find that in general, reforestation and natural forest succession can contribute to the recovery of the regulatory and provisional hydrologic services provided by TDFs through increased subsurface storage (Frankie et al., 2004; Castillo et al. 2005; Chazdon, 2008; Portillo-Quintero et al. 2015; Jones et al., 2017; Portillo-Quintero & Smith, 2018; Quijas et al., 2019). In a healthy TDF, tree roots and leaf litter inputs enhance levels of soil organic matter, improve soil structure, and create preferred pathways that encourage infiltration over overland flow and rapid water loss (Wright et al., 2018). A study of rainfall and runoff in an undisturbed TDF showed that over 70% of annual rainfall infiltrates into the subsurface where it is stored and may then be accessed by vegetation through the dry period (Farrick & Branfireun, 2014). Water storage and water yield are particularly important for human populations dependent on water yield from TDFs, as well as for plants and animals reliant on stored subsurface water during the dry season.

The land use history in Bahía results in TDFs of variable ages and disturbances, and provides a particularly valuable setting to study the relationship between forest age and hydrology. Tree water source(s) and rates of transpiration affect seasonal and annual

water balances. Here, we ask where different native species, growing in forests of different ages, derive their water over wet and dry seasons. We hypothesize that in response to limited dynamic moisture storage in the thin soil, trees in all forests, but particularly in disturbed, regenerating forests (<100 years old), will rely on deeper water sources to maintain physiological function through the dry period.

We present the results of one year of frequent monitoring to explore subsurface moisture dynamics and species-specific water use strategies across primary (>100 years), secondary (30-100 years), and young (10-30 years) TDF. In this thesis we 1) captured snapshots of changes in subsurface water content with direct measurements of shallow subsurface moisture (to depths of one meter) and subsurface water availability with measurements of predawn and midday plant water potential, and 2) identified seasonal patterns in tree water use by analyzing the stable isotope composition of bulk soil and bulk saprolite moisture, rainwater, groundwater, and tree xylem water. The results of this study answer basic hydrology questions in an understudied ecoregion and will inform community efforts to resist the fragmentation of one of the few remaining TDFs in the world.

METHODS

Site Characterization and Comparison

The Ecuadorian coast is located landward of the convergence of the subducting Nazca Plate and the overriding South American Plate. The convergence of the two tectonic plates produces a compressive tectonic regime, forming high-relief valleys and hills in Bahía. The coastal cordillera surrounding Bahía experiences a mean annual temperature of approximately 25 ^{o}C and maintains substantial atmospheric humidity, >75%, (particularly on low coast mountain crests) due to persistent 'brisas' rising off the Pacific Ocean (Dodson & Gentry, 1991). Local geology is composed of massive sandstones from the upper Miocene-Pliocene Bourbon Formation overlain by Quaternary undifferentiated terraces, alluvial deposits, and silty loam soil. This study was conducted in the Cordillera del Balsamo, a local landowner-managed bio-corridor consisting of approximately 9.64 km^2 of protected TDF (Figure 4). With a volunteer force of elementary to university students, environmental activists, and local and international non-governmental organizations (including non-governmental organizations Planet Drum and Global Student Embassy), over 45,000 trees have been planted over the past 40 years in an effort to protect and expand ecological connectivity. The combined land use history of deforestation and ongoing reforestation results in a mosaic of forests at various stages of regeneration with comparatively similar soil type, altitude, slope, and aspect.

Within the Cordillera del Balsamo, this study focuses on the Punta Gorda Natural Reserve which hosts the largest and oldest TDFs in Bahía (Site 1) as well as the oldest areas of reforestation (Site 2), and on the Bosque Verde Reserve which contains many recently reforested trees (Site 3) (Figure 4, Table 1). Punta Gorda's primary forest (Site 1) is untouched by logging due to its remote and rugged location (high altitudes approx. 303 m.a.s.l.). The dangers of landslides and dense vegetative growth make Site 1 inaccessible during the wet season (January-May), which limited our measurements to May through July and December. Prior to and during the early 1900's, the lower (approx. 65 m.a.s.l.), more accessible areas of Punta Gorda Natural Reserve were deforested for agricultural use, livestock, and firewood. Today, Punta Gorda's secondary TDF (Site 2) holds a mix of old trees, such as the Ceibo (*Ceiba trichistandra*) deemed unsuitable for logging, and over 20,000 trees (approximately 30 different native species) planted within sections of recovering TDF (ages 30-100 years old). Bosque Verde is an isolated young forest growing in the Fanca neighborhood of Bahía de Caráquez. The surrounding landscape is primarily devoid of perennial vegetation, and in the dry season appears as barren, dry hills (approx. 35 m.a.s.l.). Here, nearly all of the old growth trees have been harvested for lumber and firewood and replaced with agricultural cash crops and pasture land for animals. This site contains around 4,000 reforested trees (ages 10-30 years old and approximately 30 different native species).

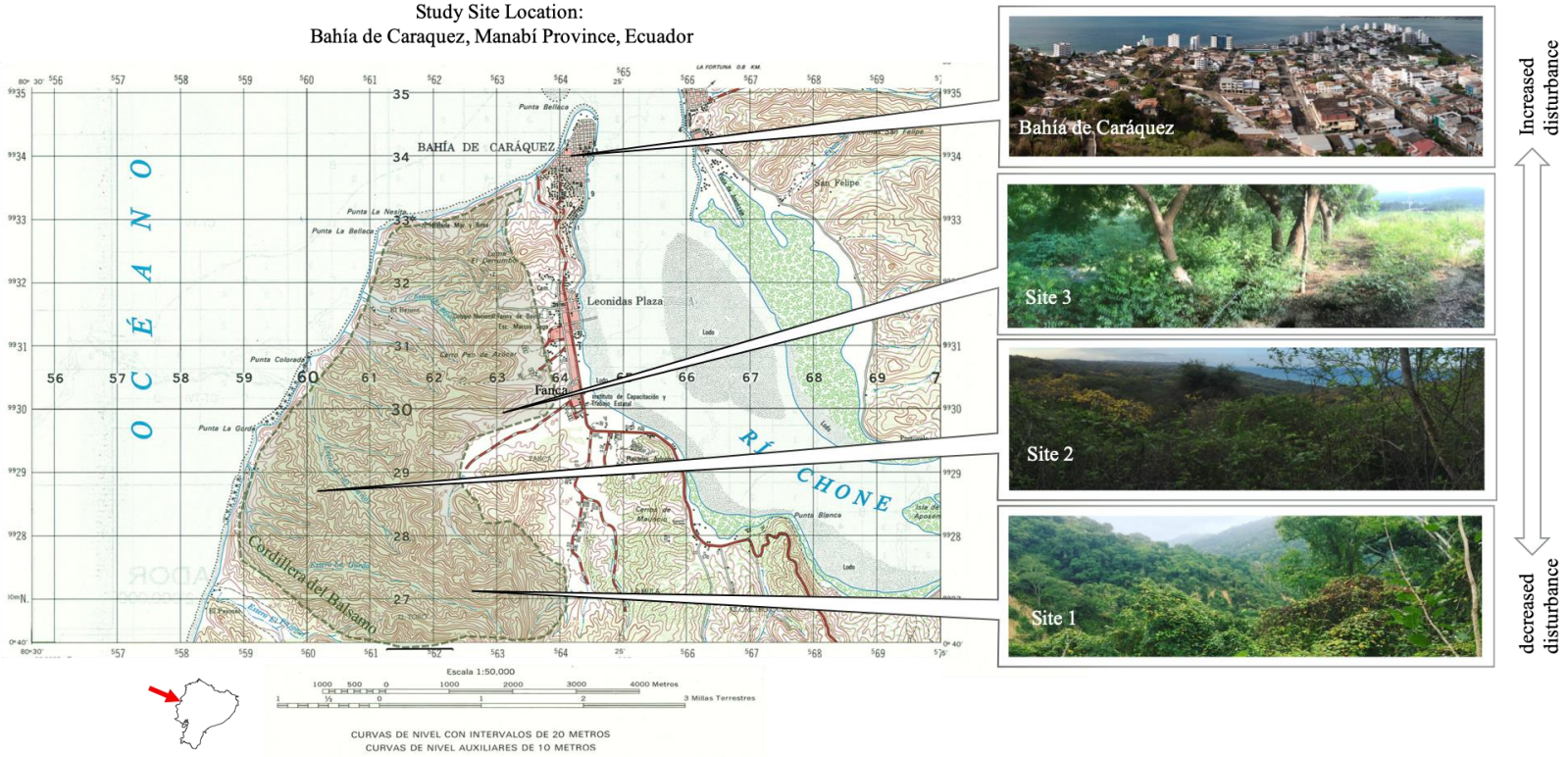

Figure 4. This study was conducted in the Cordillera del Balsamo, a local landowner managed biocorridor of protected Tropical Dry Forest (TDF). This study focuses on the Punta Gorda Natural Reserve, which hosts the largest and oldest TDFs in Bahía (Site 1) as well as the oldest areas of reforestation (Site 2), and on the Bosque Verde Reserve, which contains many

recently reforested trees despite nearly all of the old growth trees having been harvested for lumber and firewood (Site 3). Base map taken from Cañadas, L. (1983). *El mapa bioclimático y ecológico del Ecuador*.

Table 1. Cordillera del Balsamo above and belowground site comparisons:

	Site 1	**Site 2**	**Site 3**
Reserve	Punta Gorda	Punta Gorda	Bosque Verde
Elevation (m.a.s.l.)	303	65	35
Forest Age (yrs)	>100	30-100	10-30
DBH (mean ± SE) of Sampled Trees (cm)	11.72 ± 2.61	19.19 ± 3.42	19.87 ± 3.35
Dry Season Canopy Cover (%)	60.04 ± 0.16	65.90 ± 1.11	58.00 ± 2.00
Organic Matter Content (%)	5.36 ± 0.00	5.79 ± 0.00	4.14 ± 0.01
Soil Type	Silty Loam	Silty Loam	Silty Loam
Depth of Saprolite (cm)	60-80	60-70	70
Root Observations	Fine-medium roots observed between 0 and 100 cm	Fine-medium roots observed between 0 and 100 cm	Fine-medium roots observed between 0 and 100 cm

Study Tree Selection

In total, 26 trees were tagged across the sites and their species and diameter at breast height (DBH) were recorded (Table 2). Where possible, we prioritized sampling trees of the same species to increase sampling similarities across forest ages; however, many species were not found within reach and in sufficient numbers at Site 1. Furthermore, the majority of the trees at Site 1 were far too tall to sample, as their canopies were not reachable with our pruning equipment and we did not consistently climb trees to sample the canopy. Challenges of accessibility required us to focus on trees we could reach at Site 1, resulting in the notably lower Site 1 DBH distribution.

Table 2. Individual trees sampled in the Cordillera del Balsamo

Site	Common Name	Scientific Name	DBH (cm)
1	Cabo de hache	*Machaerium millei*	16.12
1	Cascol	*Caesalpinia glabrata*	6.45
1	Coca	*Sideroxylon celastrinum*	6.45
1	Guayacán	*Tabebuia chrysantha*	18.70
1	Mata palo	*Ficus obtusifolia*	24.89
1	Pela caballo	*Leucaena trichodes*	3.87
1	Secca	*Geoffroea spinosa*	10.16
1	Tillo	*Sorocea sarcocarpa*	7.09
2	Barbasco	*Jacquinia sprucei*	6.60
2	Cabo de hache	*Machaerium millei*	20.32
2	Ceibo	*Ceiba trichistandra*	53.59
2	Cereza	*Malpighia emarginata*	5.08
2	Coca	*Sideroxylon celastrinum*	10.3
2	Coca	*Sideroxylon celastrinum*	25.81
2	Coquito	*Erythoxylum glaucum*	13.21
2	Coquito	*Erythoxylum glaucum*	18.80
2	Coquito	*Erythoxylum glaucum*	22.35
2	Guayacán	*Tabebuia chrysantha*	24.64
2	Guayacán	*Tabebuia chrysantha*	21.08
2	Guayacán	*Tabebuia chrysantha*	17.78
2	Guayacán	Tabebuia chrysantha	9.91
3	Barbasco	*Jacquinia sprucei*	8.86
3	Cabo de hache	*Machaerium millei*	24.00
3	Cabo de hache	*Machaerium millei*	18.77
3	Ceibo	*Ceiba trichistandra*	13.21
3	Coquito	*Erythoxylum glaucum*	22.35
3	Guayacán	*Tabebuia chrysantha*	32.00

Campaign Timing

Bahía receives an annual average rainfall of 466 mm, 90% of which falls in January through March (WorldWeatherOnline.com). The rainless period can exceed eight months (late April throughout early December), although the common presence of a low-lying cloud cover during the dry season may limit solar radiation and temper atmospheric demand for moisture (Dodson& Gentry, 1991). Patterns in precipitation drive the timing of tree growth, green-up, and senescence in the Cordillera del Balsamo. A phenological

pattern of subsurface ‘greenness’ can be determined by using remotely sensed data to calculate the Enhanced Vegetation Index (EVI)

$$EVI = G\ x\ \frac{(\text{NIR} - \text{RED})}{(\text{NIR} + \text{C1 x RED} - \text{C2 x Blue} + \text{L})}\ x\ 100\%$$

where NIR, red, and blue correspond to specific wavelengths of reflected light corrected for atmospheric effects, L is the canopy background adjustment, and C1, C2 are coefficients of aerosol resistance (e.g., Gobron et al. 2000; Glenn et al. 2007; Huete & Glenn 2011). The range of values for EVI is -1 to 1, where healthy vegetation generally falls between values of 0.20 to 0.80 (Rankine et al., 2017). EVI will peak as forests put on new growth in response to both solar radiation and water.

In the Cordillera del Balsamo water, or water availability, is likely to control peak EVI (solar radiation remains relatively constant). We used Google Earth Engine, and geometric imports of 16-day MODIS/MCD43A4 satellite imagery polygons to produce individual EVI curves of Sites 1, 2, and 3 (Figure 5). We used seasonal trends in rainfall and the timing of peak EVI to design 11 sampling campaigns (Table 5) to: 1) capture snapshots of changes in subsurface water content with direct measurements of shallow subsurface moisture (to depths of 1 m) and water availability with measurements of predawn (Ψ_P) and midday (Ψ_M) plant water potential, and 2) identify seasonal patterns in tree water use by analyzing the stable isotope composition (δD and $\delta^{18}O$) of bulk soil and saprolite moisture, rainwater, groundwater, and tree xylem water.

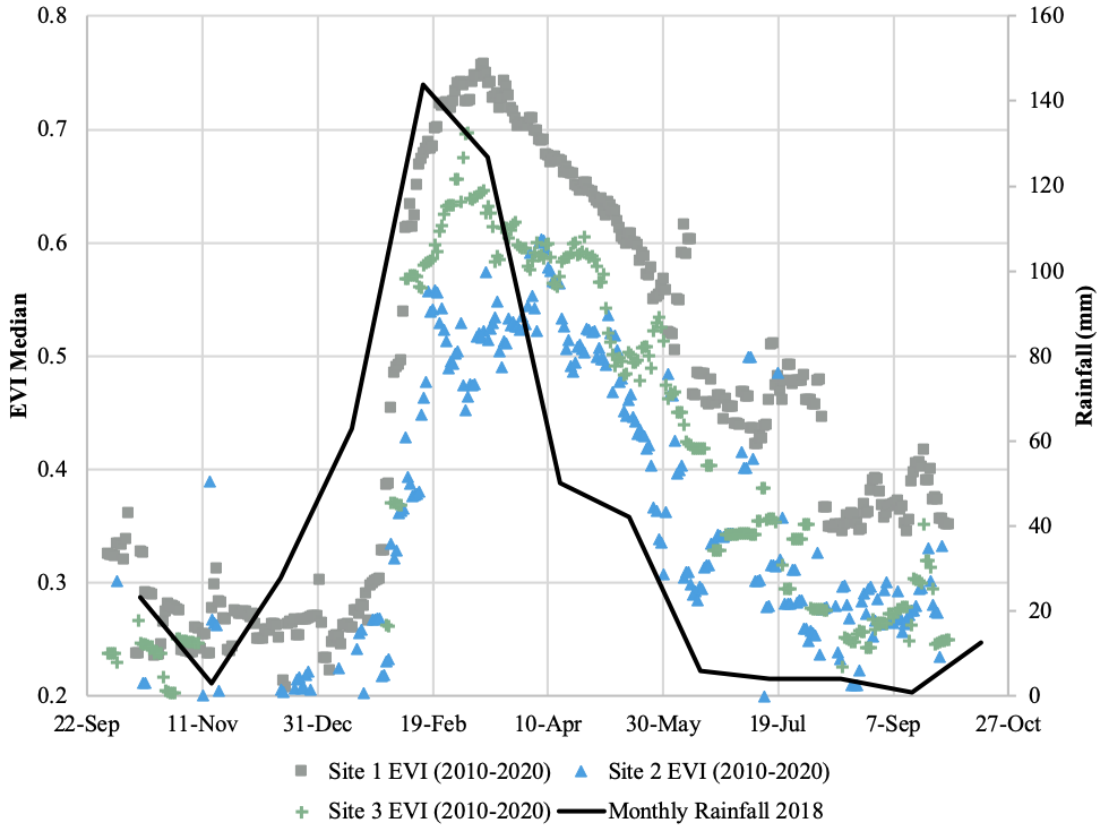

Figure 5. October 2017-2018 rainfall (WorldWeatherOnline.com) and 2010-2020 averaged MODIS/MCD43A4 remotely sensed Enhanced Vegetation Index (EVI) surface reflectance composites for Sites 1, 2, and 3. Persistent cloud cover severely limited Bahía's spatial datasets, so to keep our results robust we averaged MODIS data from 2010-2020.

Table 3. Schedule of field sampling campaigns within the Cordillera del Balsamo, Sites 1, 2 and 3

Date	Site 1	Site 2	Site 3
Dec 22-23 2017	Soil/saprolite sampled, xylem and source water collected	Soil/saprolite sampled, xylem and source water collected	-
Mar 5 2018	-	Soil/saprolite sampled, Ψ_P and Ψ_M measured, xylem and source water collected	Soil/saprolite sampled, Ψ_P and Ψ_M measured, xylem and source water collected
April 3 2018	-	Soil/saprolite sampled, xylem and source water collected	Soil/saprolite sampled, xylem and source water collected
April 19 2018	-	Soil/saprolite sampled, xylem and source water collected	Soil/saprolite sampled, xylem and source water collected
May 3 2018	-	Soil/saprolite sampled, xylem and source water collected	Soil/saprolite sampled, xylem and source water collected
May 18-19 2019	Soil/saprolite sampled, Ψ_P and Ψ_M measured, xylem and source water collected	Soil/saprolite sampled, Ψ_P and Ψ_M measured, xylem and source water collected	Soil/saprolite sampled, Ψ_P and Ψ_M measured, xylem and source water collected
May 30-June 2 2019	Soil/saprolite sampled, Ψ_P and Ψ_M measured, xylem and source water collected	Soil/saprolite sampled, Ψ_P and Ψ_M measured, xylem and source water collected	Soil/saprolite sampled, Ψ_P and Ψ_M measured, xylem and source water collected
June 12-14 2019	Soil/saprolite sampled, Ψ_P and Ψ_M measured, xylem and source water collected	Soil/saprolite sampled, Ψ_P and Ψ_M measured, xylem and source water collected	Soil/saprolite sampled, Ψ_P and Ψ_M measured, xylem and source water collected
June 23-25 2019	Soil/saprolite sampled, Ψ_P and Ψ_M measured, xylem and source water collected	Soil/saprolite sampled, Ψ_P and Ψ_M measured, xylem and source water collected	Soil/saprolite sampled, Ψ_P and Ψ_M measured, xylem and source water collected
July 4-6 2018	Soil/saprolite sampled, Ψ_P and Ψ_M measured, xylem and source water collected	Soil/saprolite sampled, Ψ_P and Ψ_M measured, xylem and source water collected	Soil/saprolite sampled, Ψ_P and Ψ_M measured, xylem and source water collected

Date	Site 1	Site 2	Site 3
Jan 7 2019	-	Soil/saprolite sampled, Ψ_P and Ψ_M measured, xylem and source water collected	Soil/saprolite sampled, Ψ_P and Ψ_M measured, xylem and source water collected

Measurements of Soil and Saprolite Moisture Content

Bulk soil and saprolite (in situ and friable weathered bedrock with a relict rock structure) samples were collected during campaigns with a bucket auger at 10 cm intervals to a maximum depth of 100 cm. At each sampling date, one auger hole was excavated and sampled per site. Holes were made in areas with the highest density of trees intended for isotopic analysis of their xylem water. Color, field texture, observable structure, and the presence or absence of roots with depth was recorded. Penetration further than 1 m was obstructed due to subsurface density and length of auger. Immediately upon collection, bulk soil and saprolite was placed inside a plastic vial and sealed with a stopper and parafilm (Bemis Co., Neenah, WI). All solid samples were stored in a cooler until brought to the lab where they were kept in a 20 °C freezer. We extracted water from bulk soil, bulk saprolite and tree xylem via cryogenic distillation (see below). Before and after extraction, we measured the mass of the bulk soil and bulk saprolite samples. After water was extracted from bulk soil and saprolite samples, we calculated soil and saprolite moisture content as

$$\frac{(\text{wet mass} - \text{dry mass})}{\text{dry mass}} \, x \, 100\%$$

according to differences in sample mass before and after cryogenic water extraction.

Measurements of Plant Water Potential

Since the development of the pressure chamber (Scholander et al., 1965), measurements of leaf water potential have been widely used to monitor plant and subsurface water status. This particular method emerged from the Cohesion-Tension theory (Dixon & Joly, 1894) and recognition that a water potential gradient ($\Delta\Psi$) drives water from the subsurface into roots (high water potential) up through the tissues of the plant and out to the atmosphere (low water potential) (Bond et al., 2008). The amount of tension held within the water-conducting system of the tree is influenced by the water potential difference between subsurface moisture and the atmosphere. When stomata close at night, there is no movement of water, and the potential of water through the tissue of a tree equilibrates with the average water potential across the tree's active roots. Measurements of tree water potential before sunrise, when stomata are closed, thus reveal the water potential in the subsurface. In this way we can use trees as sensors to probe subsurface moisture dynamics.

During the middle of the day, as a tree transpires, stomata tend to be open and water potential in a tree drops, pulling water into roots, and driving water up through the tree to the atmosphere. Measurements of tree water potential when the sun is highest is a measure of the water potential a tree achieves in pulling in water for photosynthesis, and is a sensitive indicator of vegetation responsiveness to water availability. Under very dry daytime conditions, trees may also close stomata to prevent tree water potential from falling below a critical threshold (e.g. the point of turgor loss or the onset of xylem

embolisms) (e.g., Jackson et al. 2005). Thus, we can use diurnal cycles of water potential measured in specific trees as a metric to provide partial insight to species-specific water use strategies and hydraulic limitations.

'Predawn leaf water potential' (Ψ_P) was measured for 26 trees at times between 0300 and 0500 hrs and in replicates of three leaves per tree (which were averaged into a single value). Eight trees were sampled at Site 1, thirteen trees were sampled at Site 2, and four trees were sampled at Site 3. Measurements were made with a portable pressure chamber (Model 1000, PMS Instrument Company, Albany, OR, USA and O_2 gas, as the more standardly used N_2 gas was not readily available in Bahía. Prior to using O_2 as our gas, we made paired Y measurements using N_2 and O_2 and found no statistical difference between the two sets of measurements (data not shown, $p = 0.96$). Leaf and xylem tissue samples were obtained from tree canopies with pole pruners. Trees with canopies too high or difficult to sample were excluded from this study. While it is possible that large overstory trees may be accessing moisture differently than the ones measured in this study, measurements of such trees were beyond the scope of possibility.

To study the effects of seasonal drought on the water status of juvenile trees we measured both the predawn and the midday leaf water potentials of three different species at monthly intervals. 'Midday leaf water potential' (Ψ_M) was measured for three Site 2 common, native species (*Ceiba trichistandra*, *Sideroxylon celastrinum,* and *Tabebuia chrysantha*) between 1100 and 1300 hrs and in replicates of three leaves per tree following the same procedure as the predawn samples. Ψ_M data was collected for

additional species (see Table 2), but analysis and interpretation for each species was beyond the scope of this thesis.

Isotopic Measurement of Plant Water Source

The stable isotope composition of xylem water represents a mixture of water taken up across all of the tree's roots and can be used to identify the depth of tree source water (e.g., Ehleringer & Dawson, 1992; Dawson et al., 2002). If the isotopic compositions of different subsurface reservoirs (e.g., soil, saprolite, groundwater) are distinct, seasonal variation in the isotope composition of xylem water can reveal changes in the proportion of subsurface sources used by an individual tree (White et al., 1985). In tropical sites experiencing a prolonged dry season, evaporative enrichment (as opposed to seasonal rainfall) is the major determinant of variation in the isotopic composition of water with depth (Jackson et al., 1995, 1999; Meinzer et al., 1999). The isotopic composition of the soil water varies with depth because water near the soil surface becomes enriched in the heavier isotopes as a result of evaporative enrichment (Allison 1982; Allison and Hughes 1983).

Bulk soil and bulk saprolite samples were collected via a bucket auger at 10 cm intervals to a maximum depth of 100 cm.

Rainwater samples (n = 27) were collected as often as possible during field campaigns, and were supplemented with the help of local hikers/volunteers. Groundwater samples (n = 9) were obtained from two wells. One well was located between Punta

Gorda's primary (Site 1) and secondary (Site 2) forest (5 samples), and the other well was located adjacent to Bosque Verde's recovering secondary forest (Site 3) (4 samples).

We repeatedly sampled xylem water from across the three sites for isotopic analysis (not all trees sampled for water potential were available for us to sample for stable isotope analysis due to tree size and accessibility). Xylem was sampled in two ways: if the tree's canopy was reachable by pole pruners, suberized stem wood was clipped and cut; if the tree's canopy was unreachable, tree cores were collected from the main stem of the tree between 1 and 1.5 m from the ground using an increment borer. Immediately upon extraction of a core, all tissue external to the xylem was removed and the first 5 cm of xylem tissue was immediately placed inside a plastic vial and sealed with a stopper and Parafilm to prevent evaporation prior to vacuum distillation. Because some species of tropical trees have exceptionally hard bark and sapwood, species with tall canopies and impenetrably hard wood were excluded from this study.

Water was extracted from plant xylem and bulk soil/saprolite samples at the Center for Stable Isotope Biogeochemistry at the University of California at Berkeley using a cryogenic vacuum distillation line (100°C, 1 h) (Ehleringer et al. 2000) following the procedure of West et al. 2006. Samples were run using a hot chromium reactor unit (H/Device™) interfaced with a Thermo Delta V Plus mass spectrometer and a Thermo Gas Bench II interfaced to a Thermo Delta V Plus mass spectrometer to generate δD and $\delta^{18}O$ in permil notation relative to the internationally accepted standard (Vienna Standard Mean Oceanic Water, VSMOW):

$$\delta D \text{ or } \delta^{18}O = \left(\frac{R_{sample}}{R_{standard}} - 1\right) x\ 1{,}000\ (‰)$$

Statistical Analysis

Statistical analyses were done using JMP (SAS Institute, Cary, NC, United States). Soil and saprolite moisture data and water potential data were expressed as average ± standard error. Differences in data were tested by one-way ANOVA. We used Shapiro-Wilk goodness of fit tests to test the assumption that data were normally distributed. When this function was violated, we used Kruskal-Wallis tests to detect significant differences among groups. We used Levine and Bartlett tests to test the assumptions of equal variance among groups. When this assumption was violated, we used Welch tests to detect significant differences among groups. If significant differences among groups were found, Tukey's HSD multiple means comparisons were used to determine how groups differed. For these tests, the values $P < 0.05$ were considered statistically significant. Stable isotope data were expressed as average ± standard error and as raw data in dual isotope space.

RESULTS

Site Differences in Seasonal Moisture Dynamics

Gravimetric soil and saprolite moisture content

Soil and saprolite gravimetric moisture content steadily decreased from late March through the end of the year at Sites 1, 2, and 3 (Figure 6 and Figure 7). Dry season saprolite moisture declined more quickly at Site 2 (-0.10% moisture loss/day April 3 2018- July 4 2018) than at Site 1 (-0.05% moisture loss/day May 19, 2018- July 6, 2018) and at Site 3 (-0.03% moisture loss/day April 3, 2018- July 4, 2018). However, across all sampling periods and study sites, soil moisture and saprolite moisture levels did not significantly differ from one another ($p = 0.80$).

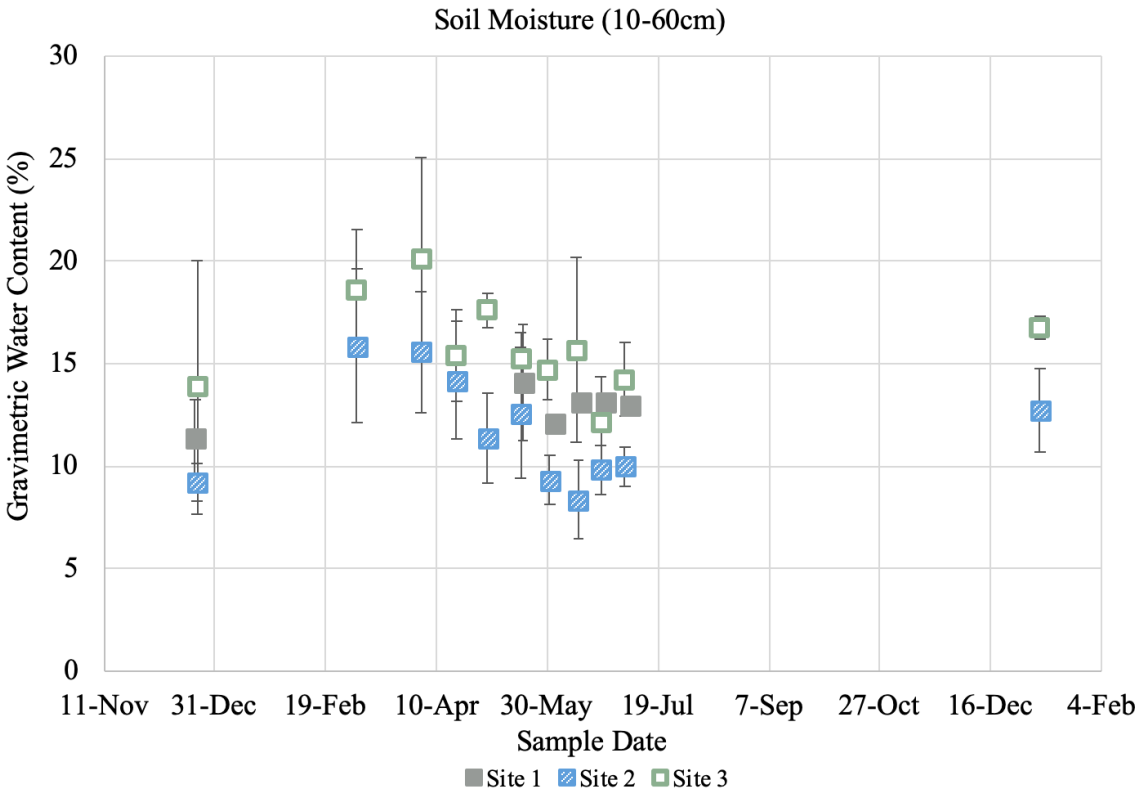

Figure 6. Soil moisture averaged at 10 cm intervals to a maximum depth of 60 cm (slight variance of depth of soil-bedrock transition across sites and sampling dates). Error bars represent standard error. Absence of Site 1 soil moisture prior to May 19, 2018 and after July 6, 2018 is due to site inaccessibility during the wet season.

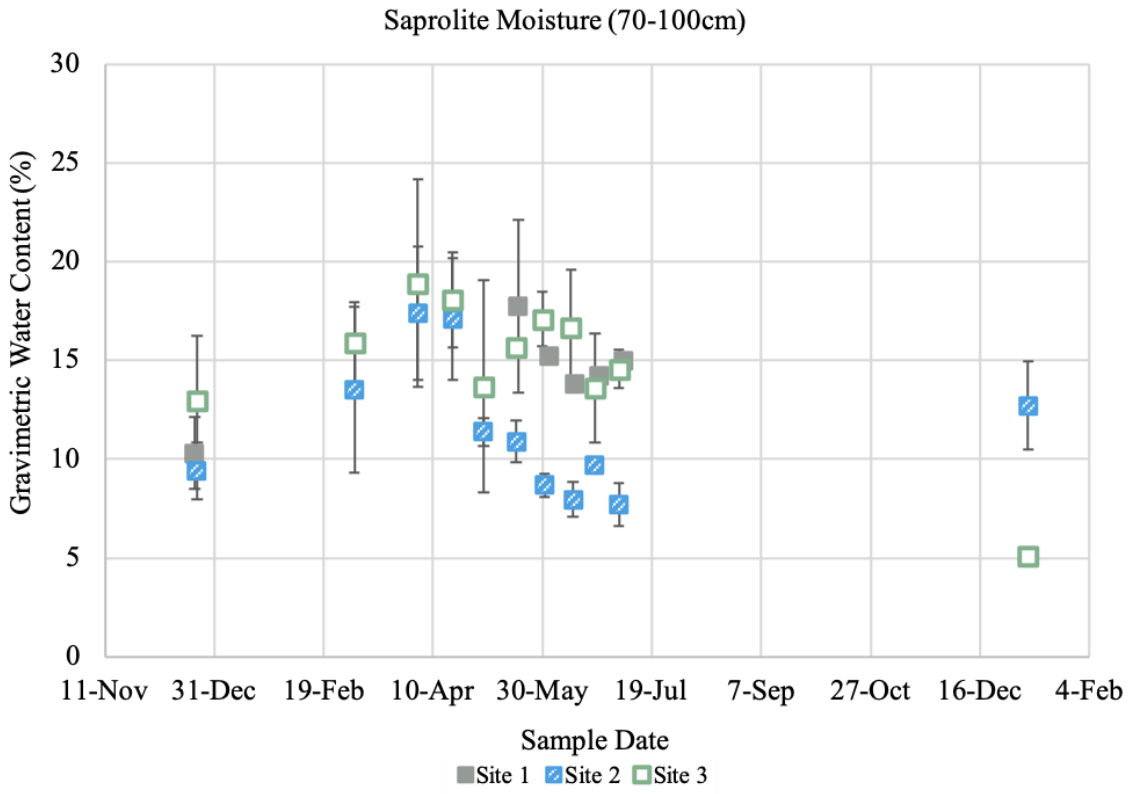

Figure 7. Saprolite moisture averaged at 10 cm intervals from 70 to 100 cm depth. Error bars represent standard error. Absence of Site 1 saprolite moisture prior to May 19, 2018 and post July 6, 2018 is due to site inaccessibility during the wet season.

We determined the total moisture lost across the dry season as the difference between maximum and minimum subsurface moisture content. We converted gravimetric measurements to volumetric water content (VWC) by estimating soil and saprolite bulk density based on observed texture. Estimates were calculated using a 1.5 g/cm^3 bulk density for silty loam soil (McKenzie et al., 2004) and a 1.68 g/cm^3 bulk density for sandstone saprolite (Wald et al., 2013). We multiplied volumetric moisture content by the

depth range of soil moisture or saprolite moisture measurements to determine mm of moisture lost. We calculated 85.75 mm, 91.42 mm, and 77.42 mm dry season moisture loss at Sites 1, 2, and 3 respectively (Table 11). Actual moisture change at Site 1, is likely to be higher because we were unable to access the site in the middle of the wet season when subsurface moisture content likely reached a maximum value. While incoming wet season rain repeatedly re-wets moisture lost due to tree water uptake, from May through December there is little to no rain input, and all changes in soil and saprolite moisture are due to evaporation and transpiration in the shallow subsurface and exclusively due to transpiration in the deeper subsurface.

Table 4. Calculated change in volumetric water content (VWC) over the top meter of soil and saprolite using maximum wet season and minimum dry season field measurements of gravimetric water content (GWC).

	Site 1		**Site 2**	**Site 3**
Change in VWC soil 19-May 2018 through 22-Dec 2018 (%)	0.03	Change in VWC soil 5-Mar 2018 through 22-Dec 2018 (mm))	0.07	0.06
Change in VWC saprolite 19-May 2018 through 22-Dec 2018 (%)	0.12	Change in VWC saprolite 5-Mar 2018 through 22-Dec 2018 (%)	0.13	0.10
Total soil moisture loss (mm)	16.27	Total soil moisture loss (mm)	39.94	37.56
Total saprolite moisture loss (mm)	49.91	Total saprolite moisture loss (mm)	51.47	39.86
Total Change (mm) of moisture in top meter	85.72	Total Change (mm) of moisture in top meter	91.42	77.42
Total Rainfall (mm) Oct 2017-2018	507.43	Total Rainfall (mm) Oct 2017-2018	507.43	507.43
Total Change as a proportion of Total Rainfall (%)	16.89	Total Change as a proportion of Total Rainfall (%)	18.01	15.25

Plant water potential

Average Ψ_P decreased at each site over the transition from wet season to dry season. Statistically significant differences between dry season group means at the $p<.05$ level was determined by one-way ANOVA (Table 5). Decreases in Ψ_P were most pronounced at Site 2 and Site 3 reaching minimum values of -1.57 ± 0.35 MPa and -2.80 ± 0.57 MPa, respectively. Contrastingly, at Site 1, the average Ψ_P never fell below -1.00 MPa (Figure 8). Sites 2 and 3 showed rapid drying between March 5, 2018 and May 31 2018. Site 2 average Ψ_P remained nearly constant from May 31, 2018 to June 23, 2018 (0.01 MPa standard deviation) but increased 0.17 MPa between late June and July 4, 2018. Average Ψ_P at Site 3 continued to decrease through early July. Sites 2 and 3 returned to high Ψ_P at the onset of the wet season in January 2019.

Table 5. Average predawn water potential (Ψ_P, MPa, mean ± SE), standard error (SE) and sample size for all Ψ_P measurements at sites 1, 2, and 3. One-way ANOVA p-values provided for comparing Ψ_P among sites within each sampling period; as applicable, sites not sharing the same letter are significantly different. Absence of Site 1 Ψ_P on March 5, 2018 and January 7, 2019 is due to site inaccessibility during the wet season. * Indicates that the data were not normally distributed and the Kruskal-Wallis test was used.

Site	**5-Mar-18**	**18-19 May 2018**	**30 May- 2 June 2018**	**12-14 June 2018**	**23-25 June 2018**	**4-Jul-18**	**7-Jan-19**
Site 1		0.45 ± 0.09 [a]	0.47 ± 0.11 [a]	0.63 ± 0.10 [a]	0.68 ± 0.15 [a]	0.76 ± 0.16 [a]	
Site 2	0.48 ± 0.06	1.15 ± 0.18 [b]	1.57 ± 0.35 [b]	1.54 ± 0.16 [b]	1.54 ± 0.38 [b]	1.38 ± 0.29 [ab]	0.53 ± 0.14
Site 3	0.48 ± 0.12	1.58 ± 0.33 [b]	1.80 ± 0.29 [ab]	1.90 ± 0.17 [b]	2.27 ± 0.43 [b]	2.80 ± 0.57 [b]	0.71 ± 0.14
p	0.94	0.01	0.003*	0.0002	0.001	0.0495*	0.48

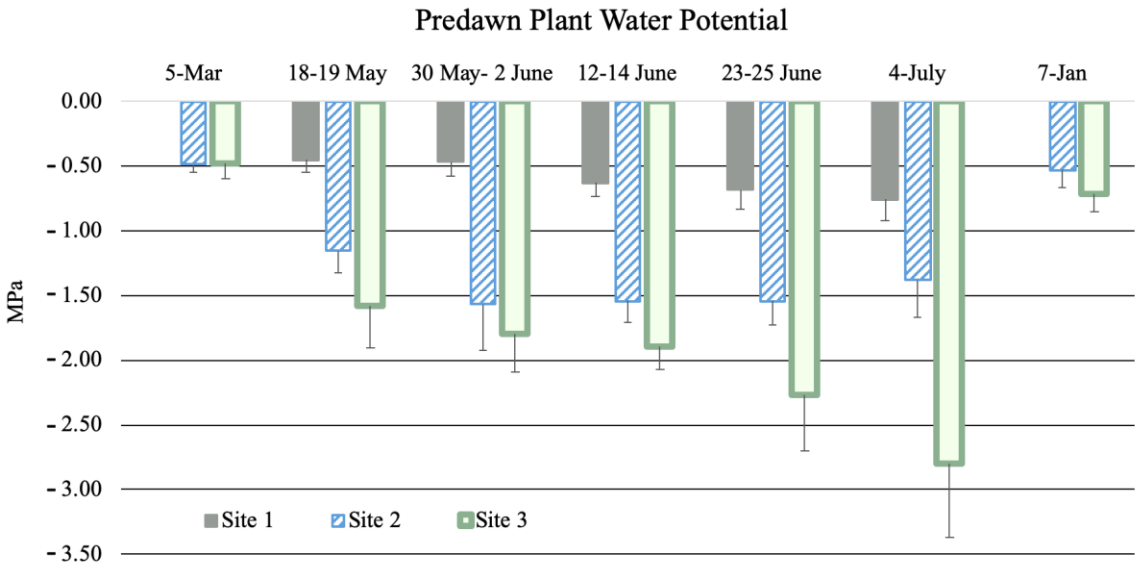

Figure 8. Mean predawn tree leaf water potential (Ψ_P). Ψ_P was measured at times between 0300 and 0500 hrs and in replicates of three leaves per tree (which were averaged into a single value). Ψ_P was averaged across individuals at each Site. Data is plotted on a non-linear x-axis. Error bars represent standard error. Absence of Site 1 Ψ_P on March 5, 2018 and January 7, 2019 is due to site inaccessibility during the wet season.

Site Trends in Plant Water Source

Isotopically characterized source water

The isotopic composition of all groundwater samples averaged -2.75 ± 0.16‰ in $\delta^{18}O$ and -11.10 ± 0.62‰ in δD. Groundwater showed little variability over time and plotted down the Global Meteoric Water Line (GMWL; a reference for plotting isotope data in dual space based on precipitation data from locations around the globe, see Figure 9) relative to the average of rainfall samples collected Dec 2017-May 2018 and January 2019 (average -2.18 ± 0.14‰ $\delta^{18}O$, -5.36 ± 0.73‰ δD) (Table 8). Using our rainfall data, we calculated a Local Meteoric Water Line (LMWL; derived from precipitation collected from a single site or set of local sites) which differed from the GMWL in slope and intercept

$$\delta D = 4.83 * \delta^{18}O + 5.12$$

We acknowledge that a more detailed sampling schedule, representative of the site-specific long-term covariation of stable isotope ratios over many years, is required for a more accurate LMWL.

At all three sites, the mean isotopic compositions of cryogenically extracted soil moisture (≤60 cm) was enriched relative to bulk saprolite moisture (≥70 cm) (Table 8). At Site 1, average bulk soil moisture (≤60 cm) $\delta^{18}O$ was -3.53 ± 0.40‰ and δD was -27.87 ± 4.31‰. Average bulk saprolite moisture (≥70 cm) $\delta^{18}O$ was -5.93± 0.49‰ and δD was 41.95 ± 4.35‰. At Site 2, average bulk soil moisture (≤60 cm) $\delta^{18}O$ was -3.56 ± 0.18‰ and δD was -29.56 ± 1.17‰. Average bulk saprolite moisture (≥70 cm) $\delta^{18}O$ was

-5.50 ± 0.30‰ and δD was -40.58 ± 2.33‰. At Site 3, average bulk soil moisture (≤60 cm) $\delta^{18}O$ was -4.06 ± 0.23‰ and δD was -29.09 ± 1.22‰. Average bulk saprolite moisture (≥70 cm) $\delta^{18}O$ was -5.97 ± 0.47‰ and δD was -41.37 ± 3.78‰.

Table 6. Comparison of average isotopic values of source water.

Sample Type	$\delta^{18}O$	SE	δD	SE	Sample Size
Rainfall	-2.18	0.26	-5.36	0.73	27
Groundwater	-2.75	0.16	-11.10	0.62	9
Site 1 Bulk Soil Moisture	-3.53	0.40	-27.87	4.31	5
Site 2 Bulk Soil Moisture	-3.56	0.18	-29.56	1.17	9
Site 3 Bulk Soil Moisture	-4.06	0.23	-29.09	1.22	9
Site 1 Bulk Saprolite Moisture	-5.93	0.49	-41.95	4.35	5
Site 2 Bulk Saprolite Moisture	-5.50	0.30	-40.58	2.33	8
Site 3 Bulk Saprolite Moisture	-5.97	0.47	-41.37	3.78	8

Isotopically characterized plant water

Isotopic analyses of xylem water show seasonal patterns in source water uptake that differ across the three sites (Table 7). At Site 1, the average isotopic composition of xylem was $\delta^{18}O$ was -3.80 ± 0.36‰ and δD was -33.10 ± 1.62‰. At Site 2, the average isotopic composition of xylem was $\delta^{18}O$ was -3.80 ± 0.24‰ and δD was -23.76 ± 1.52‰. At Site 3, the average isotopic composition of xylem was $\delta^{18}O$ was -3.46 ± 0.19‰ and δD was -17.18 ± 1.00‰. Whereas the $\delta^{18}O$ values of all three sites were remarkably similar, the average δD values were very different. Collectively, the average isotopic compositions of xylem water from each of the three sites form separate lines that are parallel to the LMWL. Site 1 xylem water data were offset from the LMWL by ~ -19.87‰ in δD, and the average isotopic composition decreased as the dry season progressed. Site 2 xylem water data were offset from the LMWL by ~ -15.56‰ in δD

and the isotope composition decreased from March 5, 2018 -May 31 2018 (wet-early dry season). However, on June 13, the average isotopic composition of Site 2 xylem water shifted towards the LMWL (offset of ~ -3.93‰ in δD). As the dry season progressed, the average isotopic composition of Site 2 individuals became more positive, moving in the direction of groundwater along a line parallel to the LMWL. Site 3 xylem water data were offset from the LMWL by ~ -5.58‰ in δD and the average isotopic composition decreased as the dry season progressed.

Table 7. Sites 1, 2 and 3 average xylem water composition, standard error, and sample size

Site	Date	$\delta^{18}O$	SE	δD	SE	Sample Size
1	Dec 22-23 2017	-4.90	0.15	-37.76	1.00	7
1	Mar 5, 2018	-	-	-	-	-
1	April 3, 2018	-	-	-	-	-
1	April 19, 2018	-	-	-	-	-
1	May 3, 2018	-	-	-	-	-
1	May 18-19, 2019	-2.49	0.44	-26.52	2.72	9
1	May 30- June 2, 2019	-3.25	0.27	-31.16	2.50	8
1	June 12-14, 2019	-3.64	0.20	-32.88	2.60	7
1	June 23-25, 2019	-3.99	0.20	-34.31	2.02	7
1	July 4-6, 2018	-4.53	0.13	-35.99	1.80	7
1	Jan 7, 2019	-	-	-	-	-
1	**Year Average**	**-3.80**	**0.19**	**-33.10**	**1.62**	**45**
2	Dec 22-23, 2017	-4.89	0.77	-26.83	5.44	7
2	Mar 5, 2018	-2.58	0.64	-19.13	2.31	9
2	April 3, 2018	-2.76	0.34	-22.29	1.52	8
2	April 19, 2018	-2.97	0.24	-23.79	1.54	8
2	May 3, 2018	-3.34	0.25	-27.95	2.68	8
2	May 18-19, 2019	-3.87	0.24	-31.39	3.07	7
2	May 30- June 2, 2019	-4.50	0.29	-31.14	4.04	8
2	June 12-14, 2019	-4.70	0.41	-22.38	1.55	8
2	June 23-25, 2019	-4.36	0.33	-21.65	1.41	8
2	July 4-6, 2018	-4.16	0.27	-18.44	1.49	8
2	Jan 7, 2019	-3.63	0.43	-16.37	2.17	8
2	**Year Average**	**-3.80**	**0.24**	**-23.76**	**1.52**	**87**
3	Dec 22-23, 2017	-	-	-	-	-
3	Mar 5, 2018	-2.29	0.88	-10.93	4.74	6
3	April 3, 2018	-2.93	0.63	-13.54	3.65	6
3	April 19, 2018	-3.43	0.43	-17.52	2.69	5
3	May 3, 2018	-3.43	0.33	-16.83	2.37	5
3	May 18-19, 2019	-3.00	0.35	-16.43	1.80	6
3	May 30- June 2, 2019	-3.84	0.56	-19.24	4.40	5
3	June 12-14, 2019	-3.59	0.62	-18.37	4.20	6
3	June 23-25, 2019	-4.40	0.92	-19.60	4.84	5
3	July 4-6, 2018	-4.11	0.74	-22.29	4.95	4
3	Jan 7, 2019	-3.55	1.09	-17.07	6.32	4
3	**Year Average**	**-3.46**	**0.19**	**-17.18**	**1.00**	**52**

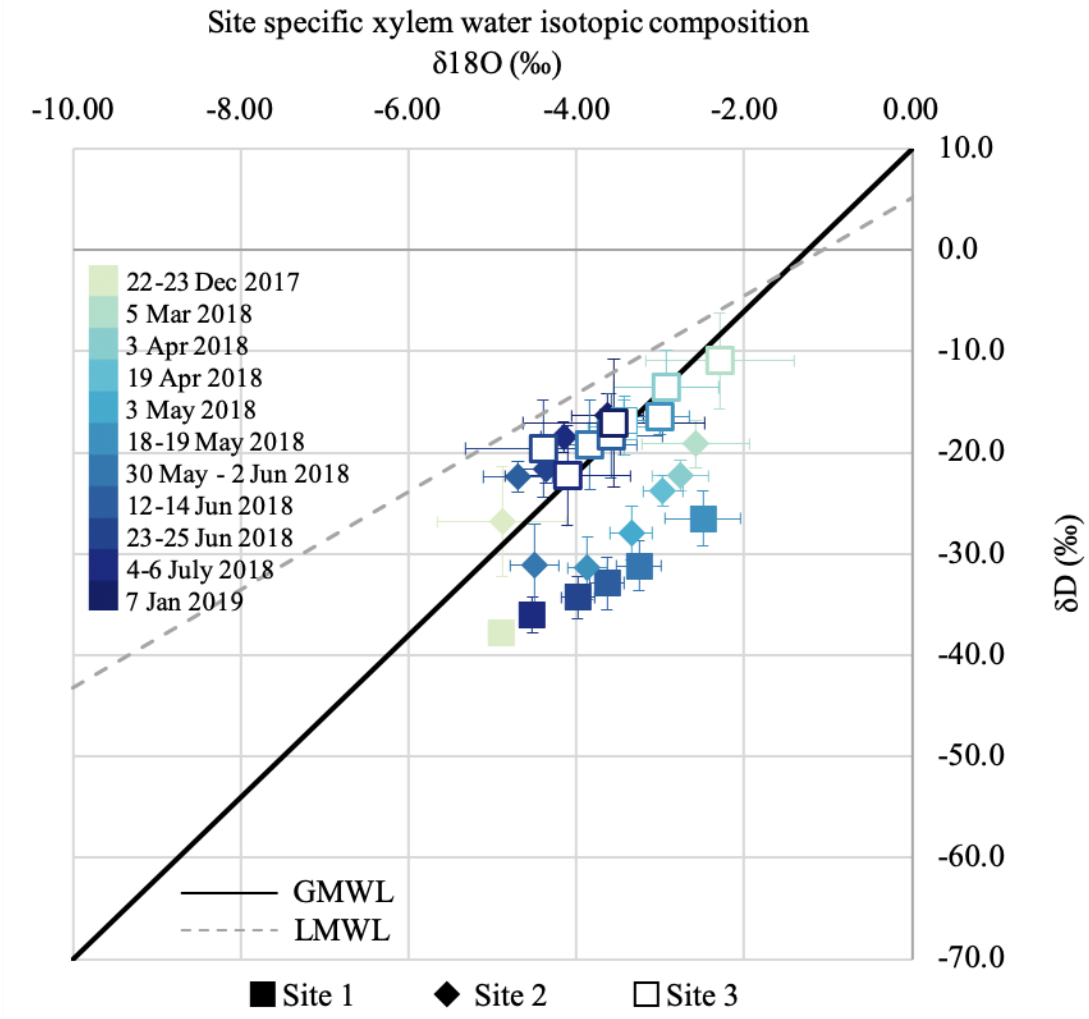

Figure 9. Site specific average xylem water composition plotted in time series with the Global Meteoric Water Line (GMWL; equation: $\delta D = 8*\delta^{18}O + 10$) and the Local Meteoric Water Line (LMWL; equation $\delta D = 4.83*\delta^{18}O + 5.11$) plotted for reference.

The relationship between tree Ψ_P and xylem water isotopic composition of tree xylem water is site-specific (Figure 10). As Ψ_P decreased, xylem water δD at Sites 1 and

3 became more negative. At Site 1, small changes in Ψ_P resulted in large changes in δD. At Site 3 large changes in Ψ_P resulted in relatively small changes in δD. At Site 2, subsurface drying from March to late-May coincided with large decreases in δD. However, beginning in late May / early June at a Ψ_P of approximately -1.57 MPa and a δD of -32 ‰, Site 2 Ψ_P and xylem water δD began to increase, arriving at -1.38 MPa and a δD of -19‰ in early July. By January 2019, both the Ψ_P and δD at Site 2 returned to values similar to January 2018.

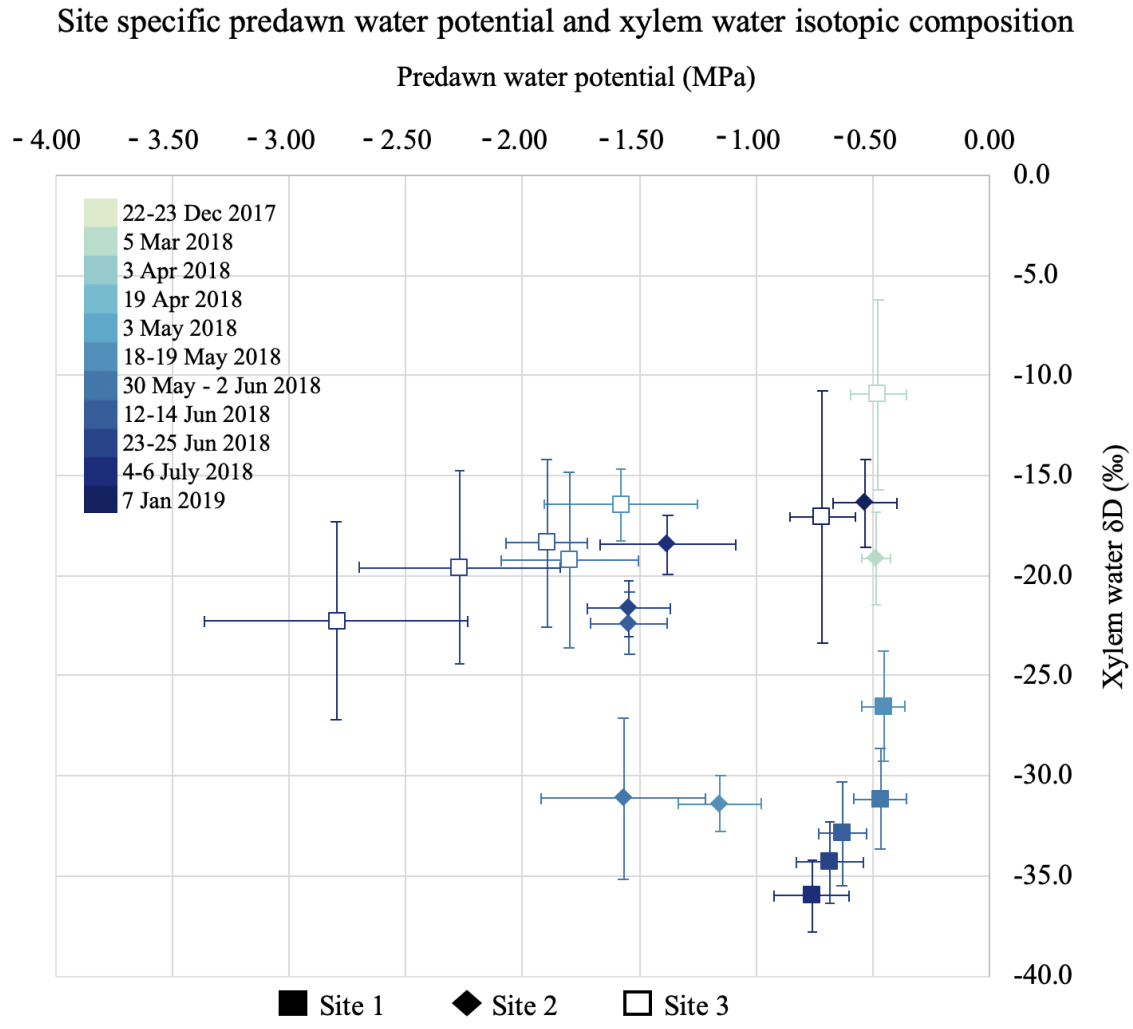

Figure 10. Average (± SE indicating variability across the species) site-specific δD xylem water composition plotted as a time series with average predawn water potential (Ψ_P). Colors indicate the date trees were sampled.

Site 1 isotopic composition of xylem water across all species

From May 2018 to July 2018 the isotopic composition of xylem water from Site 1 individuals became increasingly negative. The isotopic composition of *Ficus obtusifolia* (open circles in Figure 11) xylem water overlapped bulk soil moisture from May 19, 2018- June 25, 2018, and bulk saprolite water on July 6 2018. Several species yielded xylem waters with isotopic compositions matching no measured subsurface source. The isotopic compositions of xylem water of *Leucaena trichodes* (closed triangles in Figure 11), *Machaerium millei* (open triangles in Figure 11), *Tabebuia chrysantha* (open squares in Figure 11), *Geoffroea spinose* (closed diamonds in Figure 11), and *Sorocea sarcocarpa* (open diamonds in Figure 11) became more negative as the dry season progressed. Xylem water from these species was enriched in $\delta^{18}O$ and depleted in δD relative to bulk soil and saprolite moisture. The isotopic composition of *Caesalpinia glabrata* (closed squares in Figure 11) xylem water was more positive in $\delta^{18}O$ and more negative in δD than bulk soil and saprolite moisture during the early dry season (May 19 2018 to June 2 2018) and *Sideroxylon celastrinum* (closed circles in Figure 11) in the late dry season (June 25, 2018 to July 6, 2018).

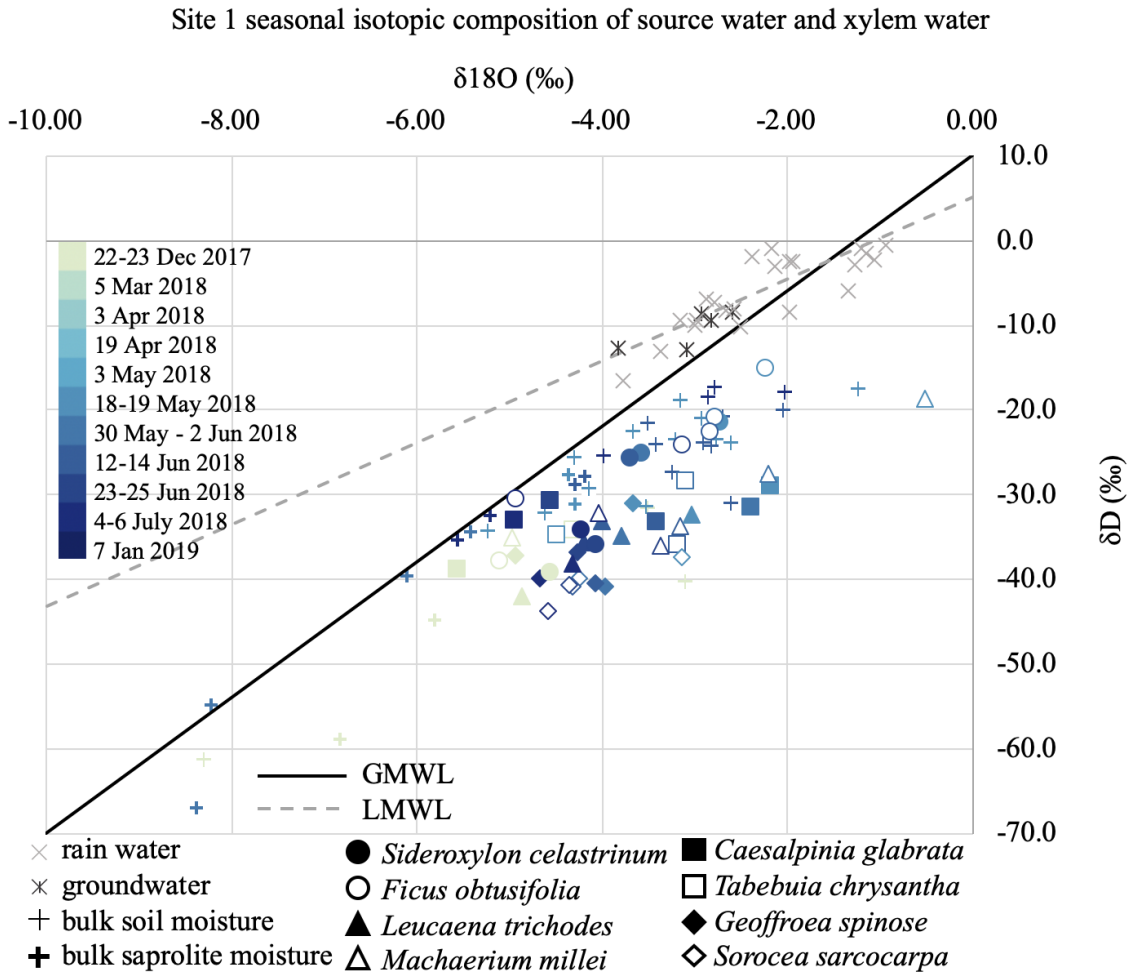

Figure 11. Site 1 xylem water isotopic compositions plotted with rainwater, groundwater, and bulk soil and bulk saprolite water. Symbols indicate the species sampled at Site 1 and the colors correspond to the sample dates. The Global Meteoric Water Line (GMWL; equation: $\delta D = 8*\delta^{18}O + 10$) and the Local Meteoric Water Line (LMWL; equation $\delta D = 4.83*\delta^{18}O + 5.11$) are plotted for reference.

Site 2 isotopic composition of xylem water across all species

From March to May the xylem water isotopic composition in Site 2 individuals became progressively more negative in a trend paralleling the LMWL. Between May 31, 2018 and June 13, 2018 there was a sudden shift in which *Jacquinia sprucei* (closed triangle in Figure 12), *Sideroxylon celastrinum* (open triangles in Figure 12), and *Tabebuia chrysantha* (open squares in Figure 12) xylem water indicated an unknown/unmeasured source water depleted in $\delta^{18}O$ and δD. From June 13, 2018 to July 4, 2018 *Jacquinia sprucei*, *Sideroxylon celastrinum* and *Tabebuia chrysantha* xylem water became more positive in a trend paralleling the LMWL. Two species deviated from this trend. Between May 31, 2018 and June 13, 2018 there was a sudden shift in which the isotopic composition of *Machaerium millei* (closed circles in Figure 12) xylem water shifted to more positive δD and $\delta^{18}O$. On June 13, 2018 the xylem water of *Machaerium millei* matched no measured subsurface source. From June 13, 2018 to July 4, 2018 *Machaerium millei* xylem water became more negative in a trend paralleling the LMWL. Uniquely, in March the isotopic composition of *Ceiba trichistandra* (open circles in Figure 12) was depleted in $\delta^{18}O$ relative to bulk saprolite moisture and plotted between saprolite moisture and the LMWL. As the dry season progressed the isotopic composition of *Ceiba trichistandra* xylem water became more positive in a trend paralleling the LMWL. By May 2018, the isotopic composition of *Ceiba trichistandra* xylem water matched groundwater, and did not change for the remainder of the sampling period.

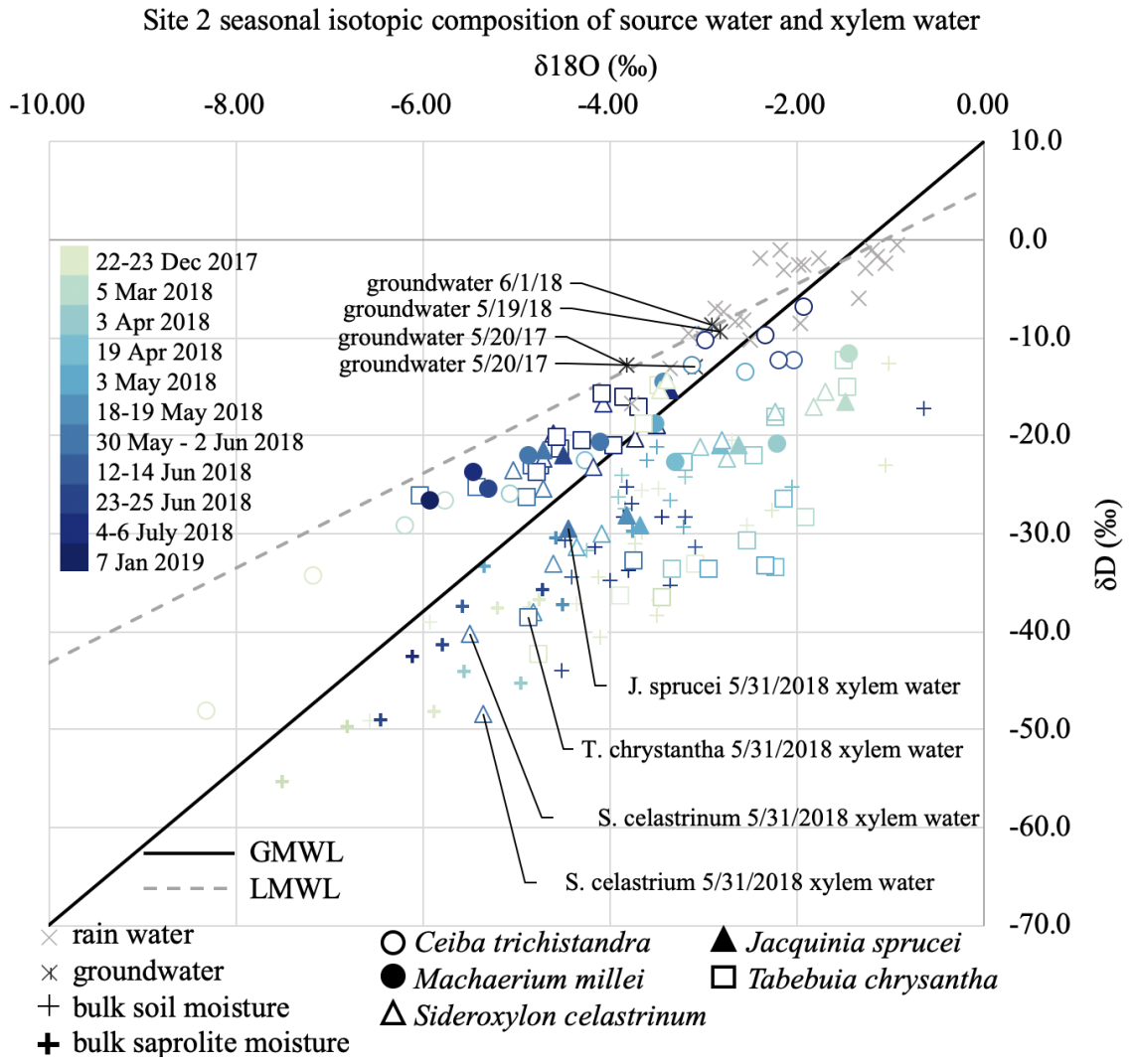

Figure 12. Site 2 xylem water isotopic compositions plotted with rainwater, groundwater, and bulk soil and bulk saprolite water. Symbols indicate the species sampled at Site 2 and the colors correspond to the sample dates. The Global Meteoric Water Line (GMWL; equation: $\delta D = 8*\delta^{18}O + 10$) and the Local Meteoric Water Line (LMWL; equation $\delta D = 4.83*\delta^{18}O + 5.11$) are plotted for reference.

Site 3 isotopic composition of xylem water across all species

From May to July 2018, the isotopic composition of average xylem water from Site 3 individuals matched no measured moisture source. Collectively, the xylem water data plotted along a line parallel to the LMWL and became more negative with time. This pattern is most clearly illustrated by species *Machaerium millei* (open triangles in Figure 13), *Tabebuia chrysantha* (open squares in Figure 13), and *Erthroxylum glaucum* (closed diamonds in Figure 13). The isotopic composition of *Machaerium millei* xylem water reached the least negative isotopic compositions as the dry season progressed, 4.44‰ $\delta^{18}O$ and, -23.8‰ δD on July 4, 2018. The isotopic composition of *Tabebuia chrysantha* xylem water reached values of -5.62 ‰ $\delta^{18}O$ and -33.8 ‰ δD on July 4 2018. Xylem water from *Erthroxylum glaucum* reached the most negative isotope compositions -7.39‰ $\delta^{18}O$ and -36.2 ‰ δD on June 23 2018. Seasonal trends in *Jacquinia sprucei* (closed triangles in Figure 13) are more difficult to discern. Site 3 *Ceiba trichistandra* (open circles in Figure 13) presented the opposite pattern, identical to Site 2 *Ceiba trichistandra*, with the isotopic composition of xylem water becoming more positive in a trend paralleling the LMWL and reflecting groundwater in the late dry season.

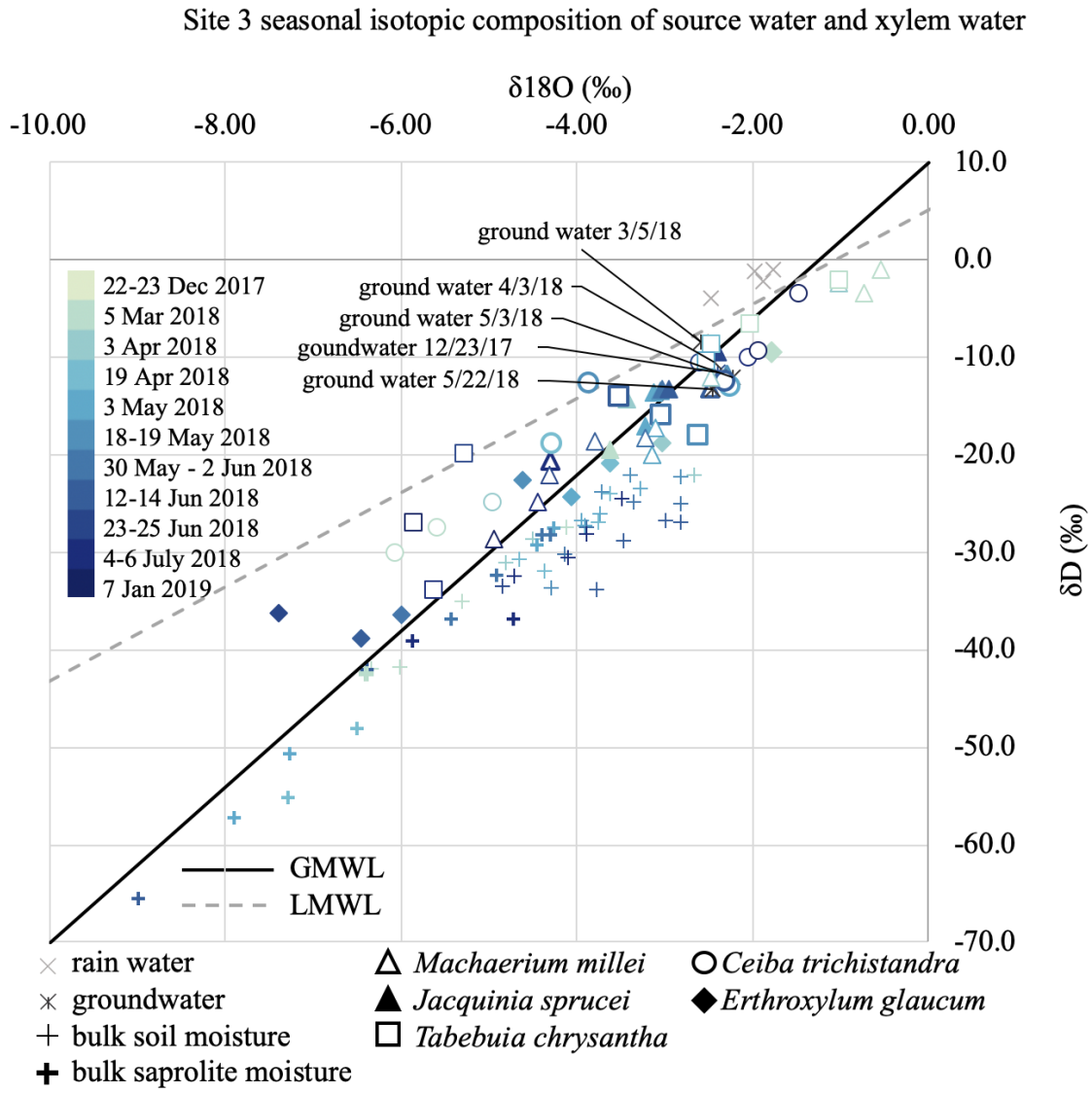

Figure 13. Site 3 seasonal xylem water isotopic compositions plotted with rainwater, groundwater, and bulk soil and bulk saprolite water. Symbols indicate the species sampled at Site 3 and the colors correspond to the sample dates. The Global Meteoric Water Line (GMWL; equation: $\delta D = 8*\delta^{18}O + 10$) and the Local Meteoric Water Line (LMWL; equation $\delta D = 4.83*\delta^{18}O + 5.11$) are plotted for reference.

Species Specific Water Use Strategies in a Regenerating Forest

The results of Ψ_P and Ψ_M measurements at Site 2 show three individuals of common, native species respond differently to drying in the subsurface. For *Ceiba trichistandra* (Figure 14, Table 8), between late May and early July (the dry season sampling period), decreases in Ψ_M tracked decreases in Ψ_P, with Ψ_M decreasing from -0.33 ± 0.15 MPa to -1.27 ± 0.21 MPa. By January 2019, *Ceiba trichistandra* Ψ_P and Ψ_M returned to water potentials similar to those measured in March 2018.

For *Sideroxylon celastrinum* (Figure 15, Table 9), in the first part of the 2018 dry season Ψ_M decreased as Ψ_P decreased. However, later in the dry season, Ψ_M increased from -3.50 ± 0.26 MPa on June 13 to -2.43 ± 0.01 MPa on June 23. Both Ψ_P and Ψ_M continued to increase through mid-July. During this time, $\Delta\Psi$ (the difference between Ψ_P and Ψ_M) decreased. Ψ_P and Ψ_M returned to values of -0.43 ± 0.31 and -0.6 ± 0.10 MPa as the dry season transitioned to the wet season in January 2019.

For *Tabebuia chrysantha* (Figure 16, Table 10), decreases in Ψ_M tracked decreases in Ψ_P, with Ψ_M decreasing from -1.23 ± 0.25 MPa to -4.30 ± 0.90 MPa between late May and early July (the dry season sampling period). By January 2019, *Tabebuia chrysantha* Ψ_P and Ψ_M returned to water potentials similar to those measured in March 2018.

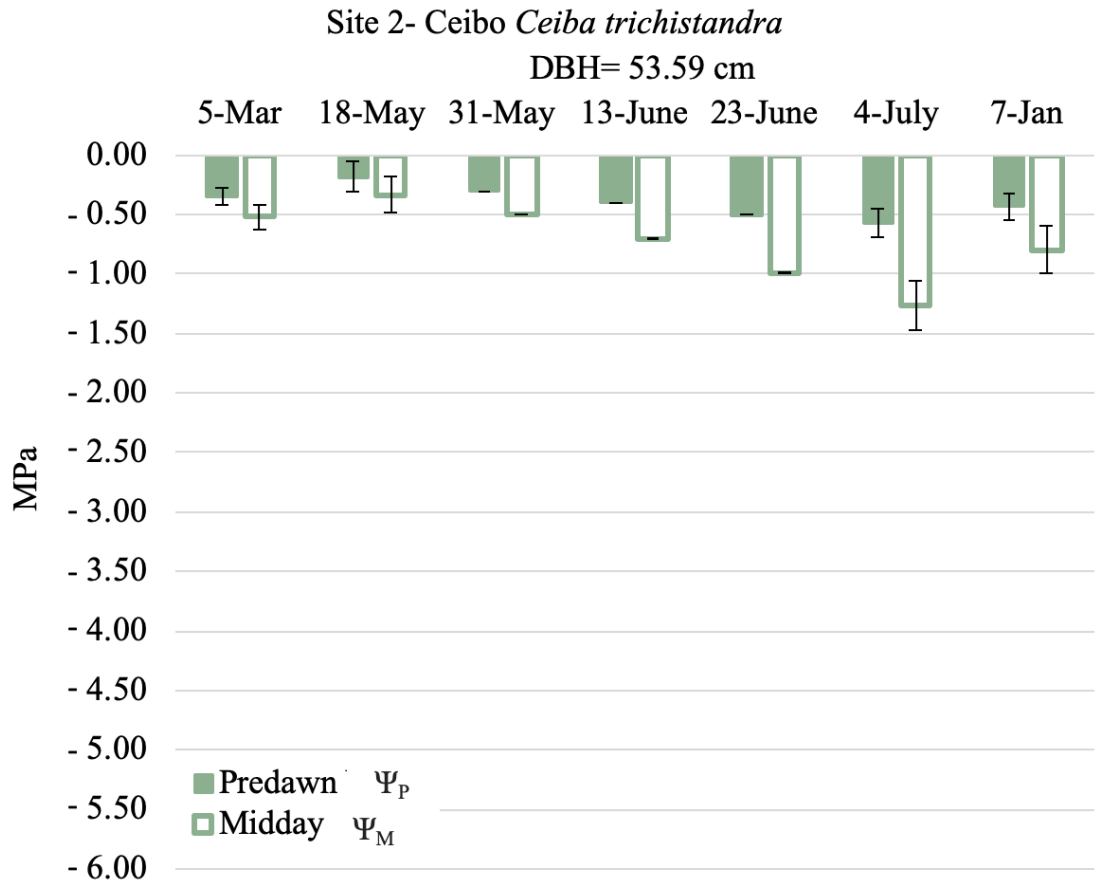

Figure 14. Predawn (Ψ_P) and midday (Ψ_M) water potential for Site 2 individual *Ceiba trichistandra* (DBH 53.59 cm). Data is plotted on a non-linear x-axis. Ψ_P was measured at times between 0300 and 0500 hrs and in replicates of three leaves per tree (which were averaged into a single value). Ψ_M was measured at times between 1100 and 1300 hrs and in replicates of three leaves per tree (which were averaged into a single value). Error bars represent standard error.

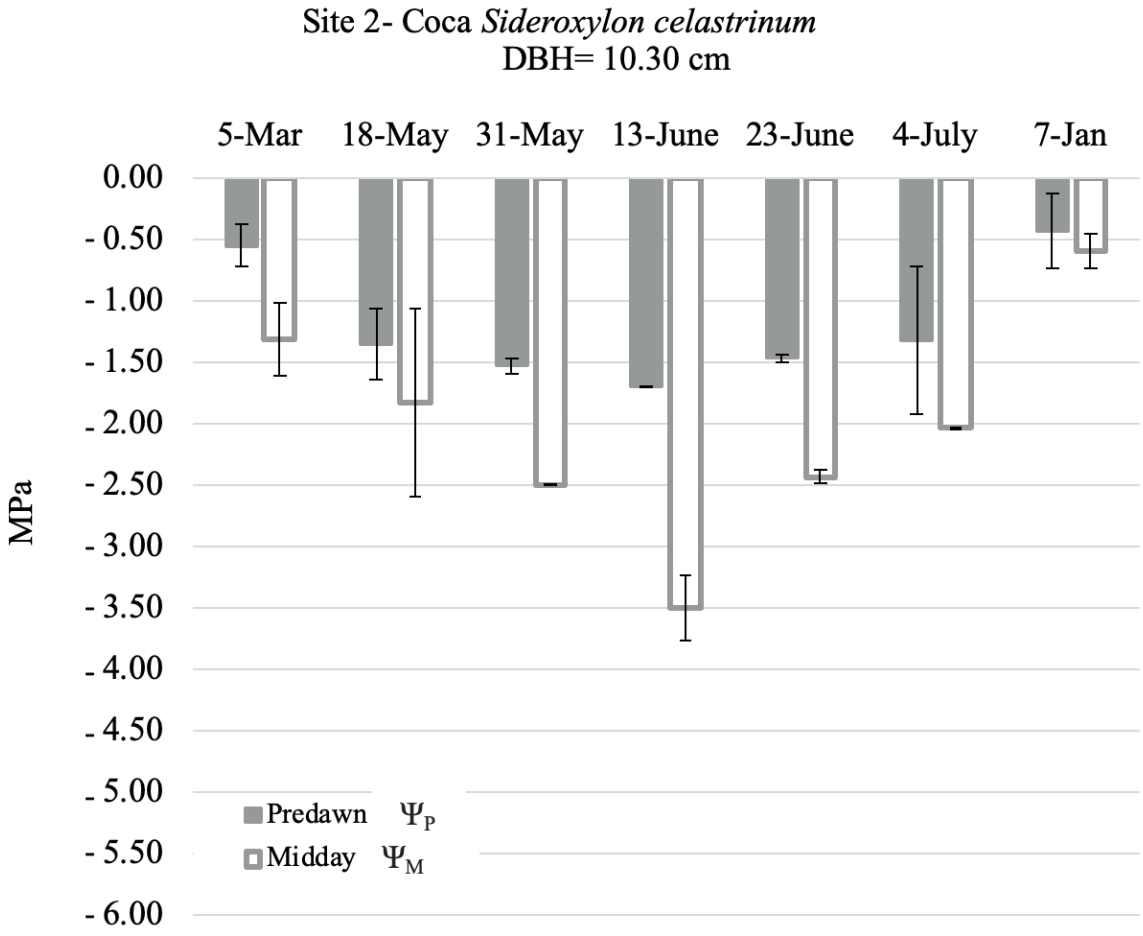

Figure 15. Predawn (Ψ_P) and midday (Ψ_M) water potential for Site 2 individual *Tabebuia chrysantha* (DBH 21.08 cm). Data is plotted on a non-linear x-axis. Ψ_P was measured at times between 0300 and 0500 hrs and in replicates of three leaves per tree (which were averaged into a single value). Ψ_M was measured at times between 1100 and 1300 hrs and in replicates of three leaves per tree (which were averaged into a single value). Error bars represent standard error.

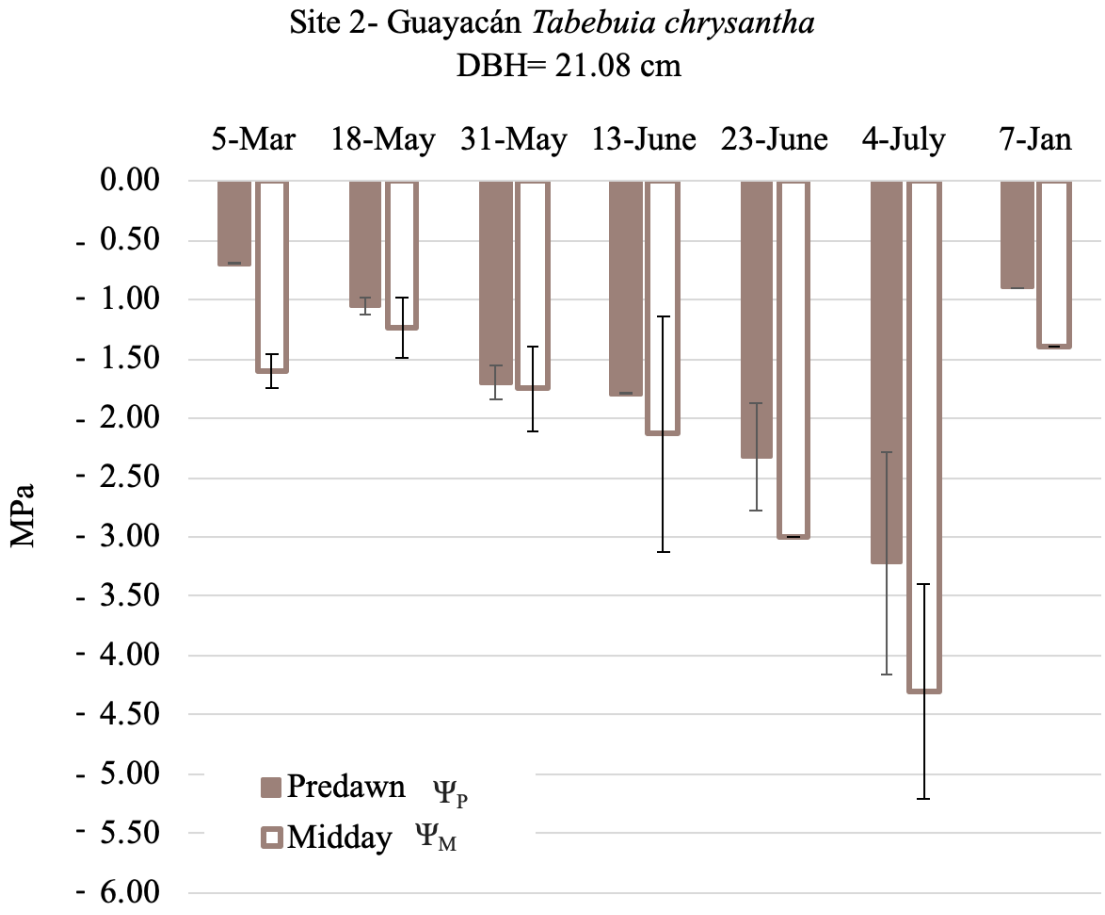

Figure 16. Predawn (Ψ_P) and midday (Ψ_M) water potential for Site 2 individual *Sideroxylon celastrinum* (DBH 10.30 cm). Data is plotted on a non-linear x-axis. Ψ_P was measured at times between 0300 and 0500 hrs and in replicates of three leaves per tree (which were averaged into a single value). Ψ_M was measured at times between 1100 and 1300 hrs and in replicates of three leaves per tree (which were averaged into a single value). Error bars represent standard error.

Table 8. *Ceiba trichistandra* averaged predawn (Ψ_P) and midday water potentials (Ψ_M) and standard error.

Date	Avg. Ψ_P (MPa)	SE	Avg. Ψ_M (MPa)	SE
5-March 2018	-0.32	0.05	-0.52	0.10
18-19 May 2018	-0.18	0.13	-0.33	0.15
30 May- 2 June 2018	-0.35	0.05	-0.50	0.05
12-14 June 2018	-0.42	0.03	-0.70	0.05
23-25 June 2018	-0.48	0.03	-0.98	0.03
4-July 2018	-0.57	0.12	-1.27	0.21
7-Jan 2019	-0.43	0.12	-0.80	0.20

Table 9. *Sideroxylon celastrinum* averaged predawn (Ψ_P) and midday water potentials (Ψ_M) and standard error.

Date	Avg. Ψ_P (MPa)	SE	Avg. Ψ_M (MPa)	SE
5-March 2018	-0.55	0.18	-1.31	0.30
18-19 May 2018	-1.36	0.29	-1.83	0.76
30 May- 2 June 2018	-1.53	0.06	-2.50	0.10
12-14 June 2018	-1.70	0.10	-3.50	0.26
23-25 June 2018	-1.47	0.03	-2.43	0.06
4-July 2018	-1.16	0.52	-2.04	0.01
7-Jan 2019	-0.43	0.31	-0.60	0.10

Table 10. *Tabebuia chrysantha* averaged predawn (Ψ_P) and midday water potentials (Ψ_M) and standard error.

Date	Avg. Ψ_P (MPa)	SE	Avg. Ψ_M (MPa)	SE
5-March 2018	-0.70	0.10	-1.60	0.10
18-19 May 2018	-1.07	0.06	-1.23	0.25
30 May- 2 June 2018	-1.70	0.10	-1.73	0.25
12-14 June 2018	-1.80	0.10	-2.13	0.99
23-25 June 2018	-2.32	0.33	-3.00	0.10
4-July 2018	-3.22	0.94	-4.30	0.90
7-Jan 2019	-0.43	0.03	-1.37	0.06

DISCUSSION

Site Differences in Subsurface Moisture Dynamics

Dry season moisture losses from soil and saprolite in the upper 1 m of the subsurface (Table 6) represent less than 20% of Bahía's 2017-2018 annual rainfall (507 mm) and are far below annual evapotranspiration estimates from TDFs (e.g., Lugo et al., 1978). Whereas we were unable to directly measure seasonal dynamics in rock moisture below a depth of 1 m, it is very likely that all species at all sites rely on deeper sources of moisture that may include groundwater and unsaturated zone rock moisture (the portion of the subsurface above the groundwater table and below the soil).

The results of the average predawn water potential measurements over the dry-out period show moisture is held at greater lower water potentials (greater tensions) in TDFs that are more-recently disturbed (<100 years old) than in old growth TDFs, in agreement with our original hypothesis. Sites 2 and 3 experienced the steepest declines in Ψ_P from wet season to dry season, and lowest average Ψ_P values (Figure 8, Table 6). These data suggest that deforestation may have altered soil and saprolite properties, and thus the moisture-tension relationship. When deforested lands are grazed, livestock trample the soil and destroy roots, which decreases aggregate stability, compacts the subsurface, and shifts pore size distribution towards smaller pores (Wright et al., 2018). Water existing in the pores of compacted soils is held at more negative matric potentials, and as a result requires more energy expenditure from a tree to access. As forests mature, their roots play an important role in disturbing the subsurface and reversing this process.

Interpretations of Site-Specific Trends in Plant Water Source

Site 1

Decreasing dry season isotopic composition of xylem water at Site 1, in conjunction with Ψ_P values that do not fall below -1.00 MPa, suggest primary forest trees use readily accessible water from progressively deeper depths, corresponding first to bulk soil moisture and then bulk saprolite moisture (Figure 9, Figure 10, Figure 11). Alone, these data imply that at Site 1 there may be sufficient moisture in the shallow subsurface to maintain forest transpiration. However, this conclusion contradicts the small quantity of moisture lost over the dry season in the upper 1 m: 85.72 mm. There is insufficient dynamic moisture storage in the upper 1 m to meet predicted transpiration from undisturbed TDFs. Furthermore, direct on-the-ground observations, and the annual EVI curve (Figure 5) show that unlike Sites 2 and 3, trees in the old growth forest at Site 1 do not lose their leaves. We provide two possible explanations. First, the elevation of the old growth forest at Site 1 (approx. 303 m.a.s.l.) may allow for condensation of 'brisas' (dry season moisture rising off of the ocean). Trees at Site 1 may access brisas through direct leaf water uptake, known as foliar uptake (Bruijnzeel, 2001; Bruijnzeel, 2004). Foliar uptake can provide additional moisture for tree growth/transpiration (~20-1900 mm/yr) (Azevedo & Morgan, 1974; del-Val et al., 2006; Ghazoul & Sheil, 2010; Bruijnzeel et al., 2011; Ellison et al., 2017). In many environments foliar uptake results in increases in Ψ_P, reflecting a hydrated plant water status decoupled from moisture tension in the subsurface (Johnson & Smith 2006; Breshears et al. 2008; Reinhardt & Smith 2008; Limm et al. 2009; Simonin et al., 2009; Kangur et al., 2017; Berry & Smith 2012; Eller et al., 2013, Eller et al., 2016; Goldsmith et al., 2013; Dawson & Goldsmith, 2018). However,

according to current literature, uptake of brisas moisture would likely reflect an enriched source water, more similar to that of rain water, not a depleted moisture source as we observed in tree xylem water at Site 1 (Berry et al., 2014).

Second, a growing body of tree source water isotope studies have documented a mismatch between xylem water and measured subsurface water sources (e.g., Lin & da SL Sternberg, 1993; Cernusak et al., 2005; Ellsworth & Williams, 2007; Eller et al., 2013; Ellsworth & Sternberg, 2015; Martín-Gómez et al., 2016; Zhao et al., 2016; Vargas et al., 2017; Barbeta et al., 2019). Tree source water isotope studies, including ours, operate on the assumption that isotope fractionation does not occur during root water uptake or during xylem transport (Zimmermann et al. 1967; Ehleringer & Dawson 1992), yet studies exist in which xylem water $\delta^{18}O$ resembles accessible moisture (held under low tension) in the soil/weathered bedrock but δD is negatively offset 10-20‰ (Brooks et al., 2010; Gierke et al., 2016; Oshun et al, 2016; Geris et al., 2017; Barbeta et al., 2019; Poca et al., 2019). Alternatively, differences between tree xylem water and source waters might occur due to fractionation along water's pathway from subsurface source through mycorrhizae into tree roots. Tree water uptake through arbuscular mycorrhizae (AMF), symbiotic associations between plant roots and soil fungi, were shown to cause negative offsets in δD (Poca et al., 2019). If AMF caused Site 1 xylem water to be negatively offset in δD (~ -19.87‰), it is possible that these trees are using a deeper water source. Mycorrhizal fungi have a widespread presence in all environments including the tropics (Fuchs & Haselwandter, 2004; Moreira et al., 2007), but documenting the relationships between Site 1 trees and mycorrhizae is beyond the scope of this thesis.

Site 2

At Site 2, the average isotopic composition in all trees, with the exception of *Ceiba trichistandra,* became progressively negative from May until June 13, 2018, plotting along measured sources of soil and saprolite moisture in dual isotope space (Figure 9, Figure 12). However, after June 13, 2018, the isotope composition of all non *Ceiba trichistandra* individuals shifted up in δD towards the LMWL and through the remainder of the dry season, increased and moved towards groundwater. The shift on June 13, 2018 was coincident with a slight relaxation in Ψ_P (Figure 10), indicating a switch to use of a more available, deep source water. We hypothesize that in response to limited dynamic moisture storage in the thin soil, trees in all forests, but particularly in disturbed, regenerating forests would rely on deeper water sources to maintain physiological function through the dry period. Together these data support our claim and suggest Site 2 individuals have access to deep, tightly held moisture sources and groundwater. The species data in Figure 12 show slight differences across three native species (including *Ceiba trichistandra*), which we explored in greater detail below.

Site 3

As the dry season progressed, there were consistent differences between the isotopic composition of xylem water from different species at Site 3. Similar to Site 2, the isotopic composition of *Ceiba trichistandra* xylem water increased as the dry season progressed, moving towards groundwater. Contrastingly, the isotopic composition of *Machaerium millei, Tabebuia chrysantha,* and *Erthroxylum glaucum,* xylem waters

decreased as the dry season progressed. Early in the dry season, the isotopic composition of xylem waters from these three species plotted near the LMWL and groundwater, more enriched than bulk soil and bulk saprolite (Figure 9, Figure 13). As the dry season progressed, the isotopic composition of these three species became progressively more negative along a line parallel to the LMWL, and matched no measured subsurface moisture source. Regrettably, our investigation of the subsurface was limited by the depth we were able to access with a hand auger (approximately 1 meter) and a point measurement of a single groundwater well. We were thus unable to document moisture and stable isotope dynamics in deeper layers of unsaturated weathered bedrock, yet unsaturated zone rock moisture can have a more negative stable isotope composition than freely mobile groundwater (Oshun et al, 2016; Rempe et al., 2018). We suggest Site 3 trees, apart from *Ceiba trichistandra*, accessed groundwater in the wet season and early part of the dry season. As the dry season progressed, these trees continued to take up water from the same depth, but a falling groundwater table beyond the rooting zone resulted in a change in source water from freely mobile groundwater to unsaturated zone rock moisture. These findings are supports by a handful of studies over the past 40 years that have highlighted the importance of moisture derived from unsaturated fractured bedrock to trees in seasonally dry environments (Arkley, 1981; Anderson et al., 1995; Zwieniecki & Newton, 1996; Hubbert et al., 2001; Hubbert et al., 2001; Rempe & Dietrich, 2018; Hahm et al., in press; Oshun et al., in prep), and more specifically in TDFs (Jackson et al. 1995; Meinzer et al. 1999; Querejeta et al. 2006, Querejeta et al., 2007; Hasselquist et al. 2010; Estrada-Medina et al., 2013).

Species-Specific Water Use Strategies in a Regenerating Forest

At Site 2, the combined results of subsurface moisture data, predawn and midday water potentials, and stable isotopes reveal three different responses to subsurface drying in three native species: *Ceiba trichistandra*, *Sideroxylon celastrinum*, and *Tabebuia chrysantha*. The water use patterns of these three species highlight three distinct strategies of sustaining hydraulic function and growth over the dry down period in the Ecuadorian TDF.

Ceiba trichistandra

From mid-May to early July, the predawn water potentials of *Ceiba trichistandra* declined, but maintained levels well above Site 2 Ψ_P averages (Figure 14). Similarly, from mid-May to early July, the midday water potentials of *Ceiba trichistandra* showed a small decline, but maintained relatively high water potentials compared to *Sideroxylon celastrinum* and *Tabebuia chrysantha*. The stable isotope data show that *Ceiba trichistandra* used a mixture of deep, unmeasured subsurface moisture (>1 meter) and groundwater as the dry season progressed. Together these results point to deep roots that enable *Ceiba trichistandra* to access sources of water held at relatively low water potentials through the dry season. In a conceptual interpretation of this data (Figure 17a) we imagine *Ceiba trichistandra* would have an advantage over shallow-rooted species by tapping into deeper sources of moisture, including groundwater, when shallow subsurface water is limited (e.g., Noy-Meir 1973). Although the maximum rooting depth of *Ceiba*

trichistandra is unknown, deep roots have been observed in a number of TDF tree species, some extending below 8 meters (e.g., Rascher et al., 2004; Maeght et al., 2013). Nevertheless, the observations in this study are supported by Zot & Winter, 1994 and Rascher, 2004 who found relatively high Ψ_P through the dry season in *Ceiba pentandra* (another species of Ceiba tree) despite declines in dry season water availability, and concluded relatively high water potentials were consistent with a deep, uninterrupted water supply throughout the year.

Notably, the genus Ceiba are typically among the tallest tropical forest species, with large umbrella-shaped canopies, bulbous green trunks, and enormous, buttressing above-ground roots. Because of their unusual trunk shape, it has long been assumed Ceiba trees depend upon stored water to survive which would suggest water use in Ceiba trees may be decoupled from drying in the subsurface. Potential stem water storage could influence Ψ_P measurements (high Ψ_P could be due to use of stored stem water rather than accessing deep water). However, recent studies of Ceiba species water use proposed that the large stem diameter of the Ceiba tree is necessary to prevent the stem from collapsing under its own mass and that the stored water may only allow for an isolated, strategic late dry season leaf flush (Chapotin et al., 2006; Butz, et al., 2018). We suggest future studies might investigate the extent that diurnal filling of *Ceiba trichistandra* stem and stored stem water isotopic composition could potentially disrupt isotopic interpretations.

Sideroxylon celastrinum

From March to mid-June the predawn and midday water potentials of *Sideroxylon celastrinum* declined, but after June 13, 2018 Ψ_P and Ψ_M increased (Figure 15). We observed no precipitation during this time period, and interpret the increase in Ψ_P and Ψ_M to be the result of a shift to a source water held at higher water potential. During this time $\Delta\Psi$ (the difference between Ψ_P and Ψ_M) decreased which may indicate stomatal sensitivity exhibited by this tree, but further interpretation is beyond the scope of this thesis. Stable isotope data show *Sideroxylon celastrinum* used moisture from bulk soil and bulk saprolite for the first part of the dry season, but by June 13th, the isotopic composition of xylem water shifted and plotted closer to the LMWL. Over the remainder of the dry season, xylem water became more positive and moved up the LMWL towards groundwater. Together, the water potential and stable isotope data suggest *Sideroxylon celastrinum* accesses deeper sources of moisture, likely unsaturated rock moisture, and proportions of groundwater late dry season.

There are two possible mechanisms by which *Sideroxylon celastrinum* may be accessing deep unsaturated rock moisture or groundwater. First, given the collection of large old growth species and younger reforested species at Site 2, we suggest larger Site 2 trees with roots in contact with deeper sources of readily accessible water may be distributing this water into drier layers in the subsurface through passive nighttime transport referred to as hydraulic lift or, hydraulic redistribution (HR) (Dawson, 1993; Burgess et al., 1998). At night, when trees close their stomata, the water potential gradient driving water from the subsurface to the canopy disappears. However, if a tree

maintains active roots in both the deep-moist and shallow-dry portions of the subsurface, a water potential gradient from high (deep and moist) to low (shallow and dry) may result in passive transport of moisture from depth to the shallow subsurface by way of tree roots. Our Ψ_P data show that *Ceiba trichistandra* roots grow in portions of the subsurface with high water potentials and the isotope data suggest that *Ceiba trichistandra* uses groundwater early in the dry season. Old growth *Ceiba trichistandra* are massive trees with some of the widest crowns in the world (up to 40 meters in crown width). If above-ground biomass serves a proxy for belowground biomass it is certainly possible a tree this size could influence deep moisture dynamics site-wide and could reasonably contribute proportions of groundwater to *Sideroxylon celastrinum*.

Second, we propose a dimorphic rooting system (Figure 17b) of shallow, lateral roots which obtain nutrients from soil layers and a taproot which accesses deep moisture and groundwater to sustain dry season growth may enable *Sideroxylon celastrinum* to access both sources of moisture (Tyree & Sperry, 1989; Dawson & Pate, 1996; Fan et al., 2017). A dimorphic rooting system with access to groundwater would explain the observed increases in Ψ_P and Ψ_M. Although *Sideroxylon celastrinum* is poorly studied, the genus *Sideroxylon* includes over 70 pantropical species, several of which have been studied extensively. For example, Chakhchar et al., 2020 observed a dimorphic root system in sub-Saharan *Sideroxylon spinosum* that seemed related to water uptake from multiple sources from different depths. In the same family, *Sapotaceae,* Oliveira et al., 2005 observed a deep dimorphic root system in Amazonian *Manilkara huberi*.

Interestingly, both studies concluded that these species facilitate the HR of water from deeper, wet layers to more shallow, dry layers during the dry season.

Tabebuia chrysantha

From mid-May to early July, predawn water potentials of *Tabebuia chrysantha* decreased to more negative values than was measured in other Site 2 species (Figure 16). *Tabebuia chrysantha* Ψ_M showed a similar decline. The water potential data suggest that *Tabebuia chrysantha*, unlike *Sideroxylon celastrinum* and *Ceiba trichistandra,* did not use deeper sources of moisture as the dry season progressed, but instead lowered Ψ_M to access a drying, and thus increasingly more tightly held, shallow water source. However, changes in the stable isotope composition of *Tabebuia chrysantha* xylem water appear to contradict the water potential data. Stable isotope data show *Tabebuia chrysantha* used moisture from bulk soil and bulk saprolite for the first part of the dry season, but by June 13th, the isotopic composition of xylem water shifted and plotted closer to the LMWL. Over the remainder of the dry season sampling, the isotopic composition of xylem water became more positive and moved up the LMWL towards groundwater. This data suggests *Tabebuia chrysantha* accesses deeper sources of moisture, likely unsaturated rock moisture, and proportions of groundwater late dry season.

To resolve these contradictory lines of evidence we offer two possible explanations. The first possibility is that, like *Sideroxylon celastrinum*, *Tabebuia chrysantha* may also possess a dimorphic rooting system which contributes to greater proportions of groundwater isotopically (Figure 17c). Unlike *Sideroxylon celastrinum*,

however, the vast majority of *Tabebuia chrysantha*'s shallow roots may remain active and continue to uptake moisture from the increasingly dry subsurface, explaining the observed decreases in Ψ_P and Ψ_M. Thus, the tap root may contribute large volumes to transpiration in *Tabebuia chrysantha*, yet its shallow roots remain functional as well. We speculate that *Tabebuia chrysantha* may have a greater need for nutrient uptake through the dry season to prepare for a flush of flowers that accompany the onset of the wet season (Tyree and Sperry, 1989). The second possibility is *Tabebuia chrysantha* may benefit from HR of deep sources of moisture (including groundwater) provided by more deeply rooted neighboring trees (such as *Ceiba trichastandra* and *Sideroxylon celastrinum*) (Figure 17d). While this would explain the contributions of groundwater recorded in *Tabebuia chrysantha*'s xylem water, HR hydration of the subsurface across *Tabebuia chrysantha*'s rooting zone is not reflected in measurements of Ψ_P and Ψ_M, and instead we see predawn and midday water potentials continue to decline. While neither possibility fully explains our data collected in this study, we conclude that *Tabebuia chrysantha* is sourcing deep moisture or groundwater either directly or indirectly.

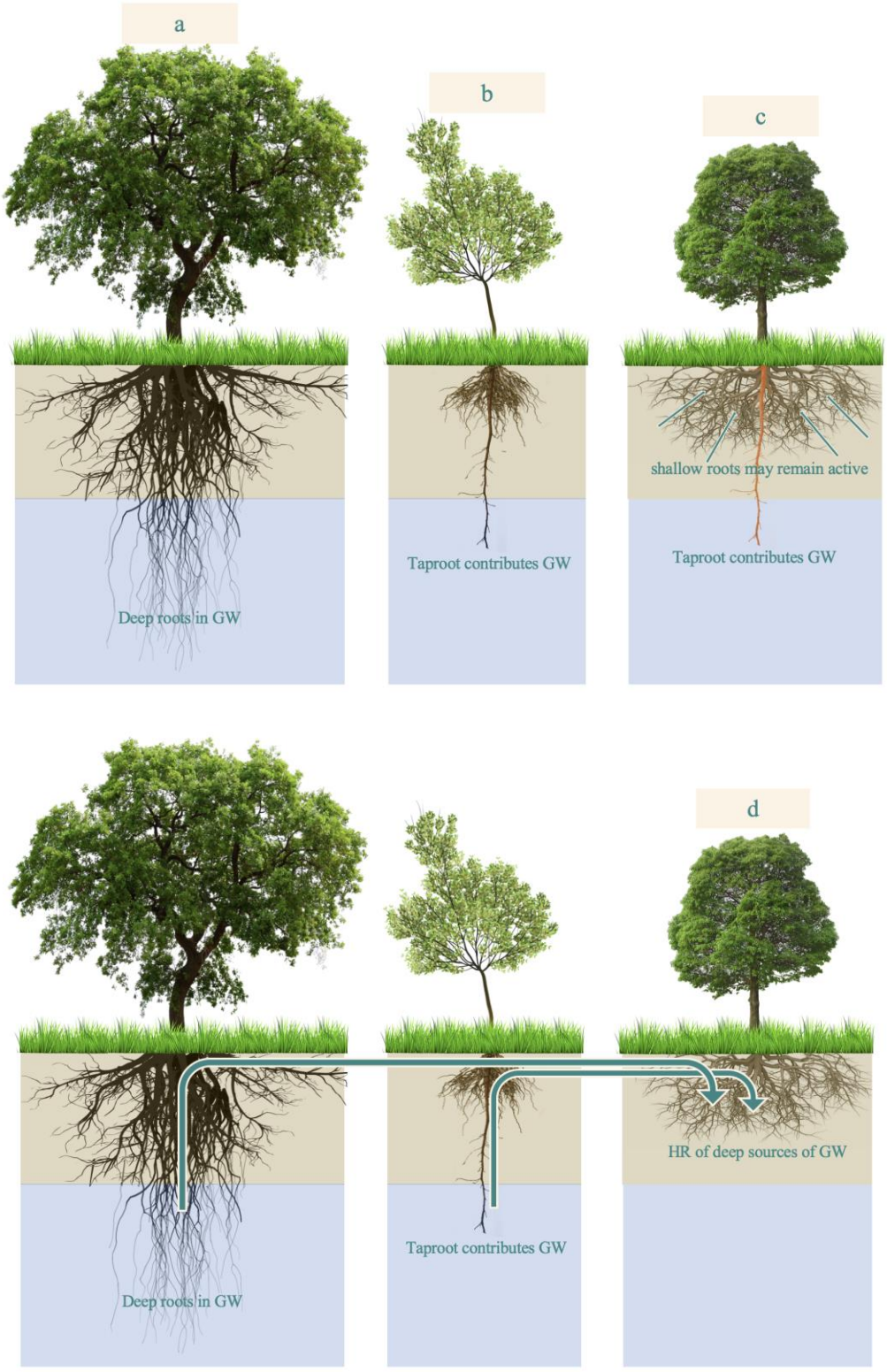
a
b
c
Deep roots in GW
Taproot contributes GW
shallow roots may remain active
Taproot contributes GW
d
Deep roots in GW
Taproot contributes GW
HR of deep sources of GW

Figure 17. At Site 2, the combined results of subsurface moisture data, predawn and midday water potentials, and stable isotopes allow us to speculate on the specific strategies utilized by TDF species to sustain hydraulic function and growth over the dry season period: **a.** *Ceiba trichistandra* likely has deep roots that enable access to consistent sources of water held at relatively low water potentials through the dry season, **b.** *Sideroxylon celastrinum* likely has a dimorphic rooting system with access to deep moisture and groundwater, **c.** *Tabebuia chrysantha* may possess active shallow subsurface roots, as well as a deep tap root which may contribute to greater proportions of groundwater isotopically **or d.** *Tabebuia chrysantha* may benefit from the hydraulic redistribution of deep sources of moisture (including groundwater) provided by more deeply rooted neighboring trees.

CONCLUSION

This study presents differences in subsurface moisture dynamics across three TDFs of contrasting ages and shows variations in tree water use that are dependent on forest age and on species-specific adaptations. We calculated 85.75 mm, 91.42 mm, and 77.42 mm dry season moisture loss in the upper 1 m at Sites 1, 2, and 3 respectively. This moisture loss is far less than expected rates of TDF transpiration, suggesting trees must be accessing rock moisture below 1 m.

Over the transition from wet season to dry season, average Ψ_P decreased at each site. Decreases in Ψ_P were most pronounced and minimum values were lowest at Site 2 and Site 3, suggesting moisture is held at greater tensions, and thus require more energy to access from trees in disturbed TDFs (<100 years old).

The results of our stable isotope monitoring uncovered age-specific differences in tree water source and confirmed our hypothesis that trees growing in regenerating forests must develop deep roots to access deep unsaturated zone rock moisture or groundwater to meet dry season moisture demands. Old growth trees may rely more heavily on foliar uptake of brisas, or may use deeper sources of moisture that are fractionated as a result of mycorrhizal-mediated water uptake. Our results highlight the importance of rock moisture, directly or indirectly sourced, across the different TDFs in Bahía and suggest that an increased capacity of roots to forage deeper for water may be a trait that enables successional species to establish under extreme seasonality and dry season conditions.

Combined results of subsurface moisture data, predawn and midday water potentials, and stable isotopes revealed secondary TDF species *Ceiba trichistandra*, *Sideroxylon celastrinum*, and *Tabebuia chrysantha* employed distinct water use strategies to survive the extended dry season. *Ceiba trichistandra* relied on a deep source of moisture held at relatively high water potentials. *Sideroxylon celastrinum* used moisture derived from the shallow subsurface through the early dry season, but switched to deeper moisture held at relatively higher water potentials in the middle of the dry season. *Sideroxylon celastrinum* may have a dimorphic rooting system that allows for water uptake of deep and shallow water sources. Predawn and midday water potential measurements show that as the dry season progressed, *Tabebuia chrysantha* continued to lower its midday water potential, relying on moisture held at low water potentials. The stable isotope data composition of *Tabebuia chrysantha* xylem water, however, reflects a shift towards deeper sources of moisture and perhaps greater contributions of groundwater in mid-summer. Whereas *Ceiba trichistandra* and *Sideroxylon celastrinum* directly use deep moisture late in the dry season, our data suggest that *Tabebuia chrysantha* relies on a tap root and shallow moisture sources, or indirectly uses deep sources of water by way of hydraulic redistribution from neighboring trees. Based on these results we suggest that on-going and future reforestation efforts prioritize a mosaic of ages and species to maximize niche partitioning of limited resources, and that these phenomena be further considered and studied with increased scientific power and scope.

This thesis contributes important autecological information for poorly studied TDF species and insight to how the distribution of individuals relates to the broader forest

community. We hope these findings will provide a foundation for future academic studies to directly aid local TDF conservation and management efforts in Bahía. But we are a long way from fully understanding the forest hydrology and ecosystem services provided by Bahía's TDF. Moving forward, we suggest there is a need to understand the extent that transpiration from regenerating forests regulates deep subsurface water storage, groundwater recharge, and forest water yield to better understand the sustainability of natural systems and water security for human communities. The results presented here may inform site specific or regional studies that quantify the effects of land use history on transpiration, subsurface water storage, groundwater recharge, and forest water yield in order to guide forest regeneration while achieving water security for human communities.

REFERENCES

Allison, G. B. (1982). The relationship between ^{18}O and deuterium in water in sand columns undergoing evaporation. *Journal of Hydrology*, *55*(1), 163–169. https://doi.org/10.1016/0022-1694(82)90127-5

Allison, G. B., & Hughes, M. H. (1983). The use of natural tracers as indicators of soil water movement in a temperate semi- arid region. *Journal of Hydrology*, *60*, 157 173.

Anderson, M. A., Graham, R. C., Alyanakian, G. J., & Martynn, D. Z. (1995). Late summer water status of soils and weathered bedrock in a giant sequoia grove. *Soil Science*, *160*(6), 415–422.

Arkley, R. J. (1981). Soil moisture use by mixed conifer forest in a summer-dry climate. *Soil Science Society of America Journal*, *45*(2), 423–427. https://doi.org/10.2136/sssaj1981.03615995004500020037x

Azevedo, J., & Morgan, D. L. (1974). Fog precipitation in coastal california forests. *Ecology*, *55*(5), 1135–1141. https://doi.org/10.2307/1940364

Bahia de Caraquez Monthly Climate Averages. (n.d.). WorldWeatherOnline.Com. Retrieved May 31, 2020, from https://www.worldweatheronline.com/lang/en-us/bahia-de-caraquez-weather/manabi/ec.aspx

Banda-R, K., Delgado-Salinas, A., Dexter, K. G., Linares-Palomino, R., Oliveira-Filho, A., Prado, D., Pullan, M., Quintana, C., Riina, R., M, G. M. R., Weintritt, J., Acevedo-Rodríguez, P., Adarve, J., Álvarez, E., B, A. A., Arteaga, J. C., Aymard,

G., Castaño, A., Ceballos-Mago, Pennington, R. T. (2016). Plant diversity patterns in neotropical dry forests and their conservation implications. *Science*, *353*(6306), 1383–1387. https://doi.org/10.1126/science.aaf5080

Barbeta, A., Jones, S. P., Clavé, L., Wingate, L., Gimeno, T. E., Fréjaville, B., Wohl, S., & Ogée, J. (2019). Unexplained hydrogen isotope offsets complicate the identification and quantification of tree water sources in a riparian forest. *Hydrology and Earth System Sciences*, *23*(4), 2129–2146. https://doi.org/10.5194/hess-23-2129-2019

Berry, Z. C., & Smith, W. K. (2012). Cloud pattern and water relations in *Picea rubens* and *Abies fraseri*, southern Appalachian Mountains, USA. *Agricultural and Forest Meteorology*, *162–163*, 27–34. https://doi.org/10.1016/j.agrformet.2012.04.005

Berry, Z. C., White, J. C., & Smith, W. K. (2014). Foliar uptake, carbon fluxes and water status are affected by the timing of daily fog in saplings from a threatened cloud forest. *Tree Physiology*, *34*(5), 459–470. https://doi.org/10.1093/treephys/tpu032

Berry, Z. C., Hughes, N. M., & Smith, W. K. (2014). Cloud immersion: An important water source for spruce and fir saplings in the southern Appalachian Mountains. *Oecologia*, *174*(2), 319–326. https://doi.org/10.1007/s00442-013-2770-0

Bond, B. J., Meinzer, F. C., & Brooks, J. R. (2008). How Trees Influence the Hydrological Cycle in Forest Ecosystems. In P. J. Wood, D. M. Hannah, & J. P. Sadler (Eds.), *Hydroecology and Ecohydrology* (pp. 7–35). John Wiley & Sons, Ltd. https://doi.org/10.1002/9780470010198.ch2

Borchert, R. (1994). Soil and stem water storage determine phenology and distribution of tropical dry forest trees. *Ecology*, *75*(5), 1437–1449. https://doi.org/10.2307/1937467

Borchert, R., Meyer, S. A., Felger, R. S., & Porter-Bolland, L. (2004). Environmental control of flowering periodicity in Costa Rican and Mexican tropical dry forests. *Global Ecology and Biogeography*, *13*(5), 409–425. https://doi.org/10.1111/j.1466-822X.2004.00111.x

Breshears, D. D., McDowell, N. G., Goddard, K. L., Dayem, K. E., Martens, S. N., Meyer, C. W., & Brown, K. M. (2008). Foliar absorption of intercepted rainfall improves woody plant water status most during drought. *Ecology*, *89*(1), 41–47.

Brooks, J. R., Barnard, H. R., Coulombe, R., & McDonnell, J. J. (2010). Ecohydrologic separation of water between trees and streams in a mediterranean climate. *Nature Geoscience*, *3*(2), 100–104. https://doi.org/10.1038/ngeo722

Bruijnzeel, L. A. (2001). *Hydrology of tropical montane cloud forests: A reassessment* (No. 1732-2016–140258). Land Use and Water Resources Research. https://doi.org/10.22004/ag.econ.47849

Bruijnzeel, L. A. (2004). Hydrological functions of tropical forests: Not seeing the soil for the trees? *Agriculture, Ecosystems & Environment*, *104*(1), 185–228. https://doi.org/10.1016/j.agee.2004.01.015

Bruijnzeel, L. A., Mulligan, M., & Scatena, F. N. (2011). Hydrometeorology of tropical montane cloud forests: Emerging patterns. *Hydrological Processes*, *25*(3), 465–498. https://doi.org/10.1002/hyp.7974

Bullock, S. H., Mooney, H. A., & Medina, E. (1995). *Seasonally Dry Tropical Forests*. Cambridge University Press.

Burgess, S. S. O., Adams, M. A., Turner, N. C., & Ong, C. K. (1998). The redistribution of soil water by tree root systems. *Oecologia*, *115*(3), 306–311.

Butz, P., Hölscher, D., Cueva, E., & Graefe, S. (2018). Tree water use patterns as influenced by phenology in a dry forest of southern ecuador. *Frontiers in Plant Science*, *9*. https://doi.org/10.3389/fpls.2018.00945

Buzzard, V., Hulshof, C. M., Birt, T., Violle, C., & Enquist, B. J. (2016). Re-growing a tropical dry forest: Functional plant trait composition and community assembly during succession. *Functional Ecology*, *30*(6), 1006–1013. https://doi.org/10.1111/1365-2435.12579

Calvo-Rodriguez, S., Sanchez-Azofeifa, A. G., Duran, S. M., & Espírito-Santo, M. M. (2017). Assessing ecosystem services in Neotropical dry forests: A systematic review. *Environmental Conservation*, *44*(1), 34–43. https://doi.org/10.1017/S0376892916000400

Cañadas, L. (1983). *El mapa bioclimático y ecológico del Ecuador*. Mag-Pronareg.

Castillo, A., Magaña, A., Pujadas, A., Martínez, L., & Godínez, C. (2005). Understanding the interaction of rural people with ecosystems: A case study in a tropical dry forest of Mexico. *Ecosystems*, *8*(6), 630–643.

Cernusak, L. A., Farquhar, G. D., & Pate, J. S. (2005). Environmental and physiological

controls over oxygen and carbon isotope composition of Tasmanian blue gum, *Eucalyptus globulus*. *Tree Physiology*, *25*(2), 129–146. https://doi.org/10.1093/treephys/25.2.129

Chakhchar, A., Lamaoui, M., Kharrassi, Y. E., Bourhim, T., Filali-Maltouf, A., & Modafar, C. E. (2020). A Review on the root system of *Argania spinosa*. *Current Agriculture Research Journal*, *8*(1), 07–17. https://doi.org/10.12944/CARJ.8.1.03

Chapotin, S. M., Razanameharizaka, J. H., & Holbrook, N. M. (2006). Water relations of baobab trees (*Adansonia* spp. L.) during the rainy season: Does stem water buffer daily water deficits? *Plant, Cell & Environment*, *29*(6), 1021–1032. https://doi.org/10.1111/j.1365-3040.2005.01456.x

Chazdon, R. L. (2008). Beyond deforestation: restoring forests and ecosystem services on degraded lands. *Science*, *320*(5882), 1458–1460.

Dawson, T. E. (1993). Hydraulic lift and water use by plants: implications for water balance, performance and plant-plant interactions. *Oecologia*, *95*(4), 565–574.

Dawson, T. E., & Ehleringer, J. R. (1993). Isotopic enrichment of water in the "woody" tissues of plants: Implications for plant water source, water uptake, and other studies which use the stable isotopic composition of cellulose. *Geochimica et Cosmochimica Acta*, *57*(14), 3487–3492. https://doi.org/10.1016/0016-7037(93)90554-A

Dawson, T. E., & Goldsmith, G. R. (2018). The value of wet leaves. *New Phytologist*, *219*(4), 1156–1169. https://doi.org/10.1111/nph.15307

Dawson, T. E., Mambelli, S., Plamboeck, A. H., Templer, P. H., & Tu, K. P. (2002).

Stable Isotopes in Plant Ecology. *Annual Review of Ecology and Systematics*, *33*, 507–559.

Dawson, T. E., & Pate, J. S. (1996). Seasonal water uptake and movement in root systems of Australian phraeatophytic plants of dimorphic root morphology: A stable isotope investigation. *Oecologia*, *107*(1), 13–20. https://doi.org/10.1007/BF00582230

del-Val, E., Armesto, J. J., Barbosa, O., Christie, D. A., Gutiérrez, A. G., Jones, C. G., Marquet, P. A., & Weathers, K. C. (2006). Rain forest islands in the Chilean semiarid region: fog-dependency, ecosystem persistence and tree regeneration. *Ecosystems*, *9*(4), 598–608.

Dixon, H. H., & Joly, J. (1894). On the ascent of sap. [Abstract]. *Proceedings of the Royal Society of London*, *57*, 3–5.

Dodson, C. H., & Gentry, A. H. (1991). Biological extinction in western Ecuador. *Annals of the Missouri Botanical Garden*, *78*(2), 273–295. https://doi.org/10.2307/2399563

Ehleringer, J. R., & Dawson, T. E. (1992). Water uptake by plants: Perspectives from stable isotope composition. *Plant, Cell & Environment*, *15*(9), 1073–1082. https://doi.org/10.1111/j.1365-3040.1992.tb01657.x

Ehleringer, J. R., Roden, J., & Dawson, T. E. (2000). Assessing ecosystem-level water relations through stable isotope ratio analyses. In O. E. Sala, R. B. Jackson, H. A. Mooney, & R. W. Howarth (Eds.), *Methods in Ecosystem Science* (pp. 181–198). Springer New York. https://doi.org/10.1007/978-1-4612-1224-9_13

Eller, C. B., Lima, A. L., & Oliveira, R. S. (2013). Foliar uptake of fog water and transport belowground alleviates drought effects in the cloud forest tree species, *Drimys brasiliensis* (Winteraceae). *New Phytologist*, *199*(1), 151–162. https://doi.org/10.1111/nph.12248

Eller, C. B., Lima, A. L., & Oliveira, R. S. (2016). Cloud forest trees with higher foliar water uptake capacity and anisohydric behavior are more vulnerable to drought and climate change. *New Phytologist*, *211*(2), 489–501. https://doi.org/10.1111/nph.13952

Ellison, D., Morris, C. E., Locatelli, B., Sheil, D., Cohen, J., Murdiyarso, D., Gutierrez, V., Noordwijk, M. van, Creed, I. F., Pokorny, J., Gaveau, D., Spracklen, D. V., Tobella, A. B., Ilstedt, U., Teuling, A. J., Gebrehiwot, S. G., Sands, D. C., Muys, B., Verbist, B., Springgay, E., Sugandi, Y., Sullivan, C. A. (2017). Trees, forests and water: Cool insights for a hot world. *Global Environmental Change*, *43*, 51–61. https://doi.org/10.1016/j.gloenvcha.2017.01.002

Ellsworth, P. Z., & Sternberg, L. S. L. (2015). Seasonal water use by deciduous and evergreen woody species in a scrub community is based on water availability and root distribution. *Ecohydrology*, *8*(4), 538–551. https://doi.org/10.1002/eco.1523

Ellsworth, P. Z., & Williams, D. G. (2007). Hydrogen isotope fractionation during water uptake by woody xerophytes. *Plant and Soil*, *291*(1–2), 93–107. https://doi.org/10.1007/s11104-006-9177-1

Estrada-Medina, H., Santiago, L. S., Graham, R. C., Allen, M. F., & Jiménez-Osornio, J.

J. (2013). Source water, phenology and growth of two tropical dry forest tree species growing on shallow karst soils. *Trees*, *27*(5), 1297–1307. https://doi.org/10.1007/s00468-013-0878-9

Fan, Y., Miguez-Macho, G., Jobbágy, E. G., Jackson, R. B., & Otero-Casal, C. (2017). Hydrologic regulation of plant rooting depth. *Proceedings of the National Academy of Sciences*, *114*(40), 10572–10577. https://doi.org/10.1073/pnas.1712381114

Farrick, K. K., & Branfireun, B. A. (2014). Infiltration and soil water dynamics in a tropical dry forest: It may be dry but definitely not arid. *Hydrological Processes*, *28*(14), 4377–4387. https://doi.org/10.1002/hyp.10177

Frankie, G. W., Mata, A., & Vinson, S. B. (2004). *Biodiversity conservation in Costa Rica: learning the lessons in a seasonal dry forest*. University of California Press.

Fuchs, B., & Haselwandter, K. (2004). Red list plants: Colonization by arbuscular mycorrhizal fungi and dark septate endophytes. *Mycorrhiza*, *14*(4), 277–281. https://doi.org/10.1007/s00572-004-0314-5

Geris, J., Tetzlaff, D., McDonnell, J. J., & Soulsby, C. (2017). Spatial and temporal patterns of soil water storage and vegetation water use in humid northern catchments. *Science of The Total Environment*, *595*, 486–493. https://doi.org/10.1016/j.scitotenv.2017.03.275

Ghazoul, J., & Sheil, D. (2010). *Tropical Rain Forest Ecology, Diversity, and Conservation*. Oxford University Press.

Gierke, C., Newton, B. T., & Phillips, F. M. (2016). Soil-water dynamics and tree water

uptake in the Sacramento Mountains of New Mexico (USA): A stable isotope study. *Hydrogeology Journal*, *24*(4), 805–818. https://doi.org/10.1007/s10040-016-1403-1

Gillespie, T. W., Lipkin, B., Sullivan, L., Benowitz, D. R., Pau, S., & Keppel, G. (2012). The rarest and least protected forests in biodiversity hotspots. *Biodiversity and Conservation*, *21*(14), 3597–3611. https://doi.org/10.1007/s10531-012-0384-1

Glenn, E. P., Huete, A. R., Nagler, P. L., Hirschboeck, K. K., & Brown, P. (2007). Integrating remote sensing and ground methods to estimate evapotranspiration. Crit. Rev. *In Plant Sciences*, 2007.

Gobron, N., Widlowski, J.-L., Verstraete, M. M., & Pinty, B. (2000). Advanced vegetation indices optimized for up-coming sensors: Design, performance, and applications. *IEEE Transactions on Geoscience and Remote Sensing*, *38*(6), 2489–2505. https://doi.org/10.1109/36.885197

Goldsmith, G. R., Matzke, N. J., & Dawson, T. E. (2013). The incidence and implications of clouds for cloud forest plant water relations. *Ecology Letters*, *16*(3), 307–314. https://doi.org/10.1111/ele.12039

Hansen, M. C., Stehman, S. V., & Potapov, P. V. (2010). Quantification of global gross forest cover loss. *Proceedings of the National Academy of Sciences*, *107*(19), 8650–8655. https://doi.org/10.1073/pnas.0912668107

Hasselquist, N. J., Allen, M. F., & Santiago, L. S. (2010). Water relations of evergreen

and drought-deciduous trees along a seasonally dry tropical forest chronosequence. *Oecologia*, *164*(4), 881–890. https://doi.org/10.1007/s00442-010-1725-y

Horstman, E. (2017). Establishing a Private Protected Area in Ecuador: Lessons learned in the management of Cerro Blanco Protected Forest in the city of Guayaquil. *Case Studies in the Environment*, *1*(1), 1–14. https://doi.org/10.1525/cse.2017.sc.452964

Hubbert, K. R., Beyers, J. L., & Graham, R. C. (2001). Roles of weathered bedrock and soil in seasonal water relations of *Pinus Jeffreyi* and *Arctostaphylos patula*. *Canadian Journal of Forest Research*, *31*(11), 1947–1957. https://doi.org/10.1139/x01-136

Hubbert, K. R., Graham, R. C., & Anderson, M. A. (2001). Soil and weathered bedrock. *Soil Science Society of America Journal*, *65*(4), 1255–1262. https://doi.org/10.2136/sssaj2001.6541255x

Jackson, P. C., Cavelier, J., Goldstein, G., Meinzer, F. C., & Holbrook, N. M. (1995). Partitioning of water resources among plants of a lowland tropical forest. *Oecologia*, *101*(2), 197–203.

Jackson, P. C., Meinzer, F. C., Bustamante, M., Goldstein, G., Franco, A., Rundel, P. W., Caldas, L., Igler, E., & Causin, F. (1999). Partitioning of soil water among tree species in a Brazilian Cerrado ecosystem. *Tree Physiology*, *19*(11), 717–724. https://doi.org/10.1093/treephys/19.11.717

Jackson, R. B., Jobbágy, E. G., Avissar, R., Roy, S. B., Barrett, D. J., Cook, C. W.,

Farley, K. A., Maitre, D. C. le, McCarl, B. A., & Murray, B. C. (2005). Trading water for carbon with biological carbon sequestration. *Science, 310*(5756), 1944–1947. https://doi.org/10.1126/science.1119282

Janzen, D. H. (1988). *Tropical Dry Forests. Biodiversity.* https://www.nap.edu/989

Johnson, D. M., & Smith, W. K. (2006). Low clouds and cloud immersion enhance photosynthesis in understory species of a southern Appalachian spruce–fir forest (USA). *American Journal of Botany*, *93*(11), 1625–1632. https://doi.org/10.3732/ajb.93.11.1625

Jones, J., Almeida, A., Cisneros, F., Iroumé, A., Jobbágy, E., Lara, A., Lima, W. de P., Little, C., Llerena, C., Silveira, L., & Villegas, J. C. (2017). Forests and water in South America. *Hydrological Processes*, *31*(5), 972–980. https://doi.org/10.1002/hyp.11035

Kangur, O., Kupper, P., & Sellin, A. (2017). Predawn disequilibrium between soil and plant water potentials in light of climate trends predicted for northern Europe. *Regional Environmental Change*, *17*(7), 2159–2168. https://doi.org/10.1007/s10113-017-1183-8

Kennard, D. K. (2002). Secondary forest succession in a tropical dry forest: Patterns of development across a 50-year chronosequence in lowland Bolivia. *Journal of Tropical Ecology*, *18*(1), 53–66.

Limm, E. B., Simonin, K. A., Bothman, A. G., & Dawson, T. E. (2009). Foliar water uptake: A common water acquisition strategy for plants of the redwood forest. *Oecologia*, *161*(3), 449–459. https://doi.org/10.1007/s00442-009-1400-3

Lugo, A. E., Gonzalez-Liboy, J. A., Cintron, B., & Dugger, K. (1978). Structure, productivity, and transpiration of a subtropical dry forest in Puerto Rico. *Biotropica*, *10*(4), 278–291. https://doi.org/10.2307/2387680

Maeght, J.-L., Rewald, B., & Pierret, A. (2013). How to study deep roots—And why it matters. *Frontiers in Plant Science*, *4*. https://doi.org/10.3389/fpls.2013.00299

Meinzer, F. C., Andrade, J. L., Goldstein, G., Holbrook, N. M., Cavelier, J., & Wright, S. J. (1999). Partitioning of soil water among canopy trees in a seasonally dry tropical forest. *Oecologia*, *121*(3), 293–301. https://doi.org/10.1007/s004420050931

Miles, L., Newton, A. C., DeFries, R. S., Ravilious, C., May, I., Blyth, S., Kapos, V., & Gordon, J. E. (2006). A global overview of the conservation status of tropical dry forests. *Journal of Biogeography*, *33*(3), 491–505.

Moreira, M., Baretta, D., Tsai, S. M., Gomes-da-Costa, S. M., & Cardoso, E. J. B. N. (2007). Biodiversity and distribution of arbuscular mycorrhizal fungi in Araucaria angustifolia forest. *Scientia Agricola*, *64*(4), 393–399. https://doi.org/10.1590/S0103-90162007000400010

Murphy, P. G., & Lugo, A. E. (1986). Ecology of Tropical Dry Forest. *Annual Review of Ecology and Systematics*, *17*(1), 67–88. https://doi.org/10.1146/annurev.es.17.110186.000435

Noy-Meir, I. (1973). Desert ecosystems: Environment and producers. *Annual Review of Ecology and Systematics*, *4*(1), 25–51. https://doi.org/10.1146/annurev.es.04.110173.000325

Oliveira, R. S., Dawson, T. E., Burgess, S. S. O., & Nepstad, D. C. (2005). Hydraulic redistribution in three Amazonian trees. *Oecologia*, *145*(3), 354–363. https://doi.org/10.1007/s00442-005-0108-2

Oshun, J., Dietrich, W. E., Dawson, T. E., & Fung, I. (2016). Dynamic, structured heterogeneity of water isotopes inside hillslopes. *Water Resources Research*, *52*(1), 164–189. https://doi.org/10.1002/2015WR017485

Oshun, J. (2016). The isotopic evolution of a raindrop through the critical zone (Doctoral dissertation, UC Berkeley).

Pennington, R. T., Lavin, M., & Oliveira-Filho, A. (2009). Woody plant diversity, evolution, and ecology in the tropics: Perspectives from seasonally dry tropical forests. *Annual Review of Ecology, Evolution, and Systematics*, *40*(1), 437–457. https://doi.org/10.1146/annurev.ecolsys.110308.120327

Plan de Desarrollo y Ordenamiento Territorial 2015—2019. (n.d.). 178.

Poca, M., Coomans, O., Urcelay, C., Zeballos, S. R., Bodé, S., & Boeckx, P. (2019). Isotope fractionation during root water uptake by *Acacia caven* is enhanced by arbuscular mycorrhizas. *Plant and Soil*, *441*(1–2), 485–497. https://doi.org/10.1007/s11104-019-04139-1

Portillo-Quintero, C. A., & Sánchez-Azofeifa, G. A. (2010). Extent and conservation of tropical dry forests in the Americas. *Biological Conservation*, *143*(1), 144–155. https://doi.org/10.1016/j.biocon.2009.09.020

Portillo-Quintero, C., Sanchez-Azofeifa, A., Calvo-Alvarado, J., Quesada, M., & do

Espirito Santo, M. M. (2015). The role of tropical dry forests for biodiversity, carbon and water conservation in the neotropics: Lessons learned and opportunities for its sustainable management. *Regional Environmental Change*, *15*(6), 1039–1049. https://doi.org/10.1007/s10113-014-0689-6

Portillo-Quintero, C., & Smith, V. (2018). Emerging trends of tropical dry forests loss in North & Central America during 2001–2013: The role of contextual and underlying drivers. *Applied Geography*, *94*, 58–70. https://doi.org/10.1016/j.apgeog.2018.03.011

Querejeta, J. I., Estrada-Medina, H., Allen, M. F., & Jiménez-Osornio, J. J. (2007). Water source partitioning among trees growing on shallow karst soils in a seasonally dry tropical climate. *Oecologia*, *152*(1), 26–36. https://doi.org/10.1007/s00442-006-0629-3

Querejeta, J. I., Estrada-Medina, H., Allen, M. F., Jiménez-Osornio, J. J., & Ruenes, R. (2006). Utilization of bedrock water by *Brosimum alicastrum* trees growing on shallow soil atop limestone in a dry tropical climate. *Plant and Soil*, *287*(1), 187. https://doi.org/10.1007/s11104-006-9065-8

Quesada, M., Sanchez-Azofeifa, G. A., Alvarez-Añorve, M., Stoner, K. E., Avila Cabadilla, L., Calvo-Alvarado, J., Castillo, A., Espírito-Santo, M. M., Fagundes, M., Fernandes, G. W., Gamon, J., Lopezaraiza-Mikel, M., Lawrence, D., Morellato, L. P. C., Powers, J. S., Neves, F. de S., Rosas-Guerrero, V., Sayago, R., & Sanchez-Montoya, G. (2009). Succession and management of tropical dry

forests in the Americas: Review and new perspectives. *Forest Ecology and Management, 258*(6), 1014–1024. https://doi.org/10.1016/j.foreco.2009.06.023

Quijas, S., Romero-Duque, L. P., Trilleras, J. M., Conti, G., Kolb, M., Brignone, E., & Dellafiore, C. (2019). Linking biodiversity, ecosystem services, and beneficiaries of tropical dry forests of Latin America: Review and new perspectives. *Ecosystem Services*, *36*, 100909. https://doi.org/10.1016/j.ecoser.2019.100909

Rankine, C., Sánchez-Azofeifa, G. A., Guzmán, J. A., Espirito-Santo, M. M., & Sharp, I. (2017). Comparing MODIS and near-surface vegetation indexes for monitoring tropical dry forest phenology along a successional gradient using optical phenology towers. *Environmental Research Letters*, *12*(10), 105007. https://doi.org/10.1088/1748-9326/aa838c

Rascher, U., Bobich, E. G., Lin, G. H., Walter, A., Morris, T., Naumann, M., Nichol, C. J., Pierce, D., Bil, K., Kudeyarov, V., & Berry, J. A. (2004). Functional diversity of photosynthesis during drought in a model tropical rainforest – the contributions of leaf area, photosynthetic electron transport and stomatal conductance to reduction in net ecosystem carbon exchange. *Plant, Cell & Environment*, *27*(10), 1239–1256. https://doi.org/10.1111/j.1365-3040.2004.01231.x

Reinhardt, K., & Smith, W. K. (2008). Impacts of Cloud Immersion on Microclimate, Photosynthesis and Water Relations of Abies fraseri (Pursh.) Poiret in a Temperate Mountain Cloud Forest. *Oecologia*, *158*(2), 229–238. JSTOR.

Rempe, D. M., & Dietrich, W. E. (2018). Direct observations of rock moisture, a hidden

component of the hydrologic cycle. *Proceedings of the National Academy of Sciences*, *115*(11), 2664–2669. https://doi.org/10.1073/pnas.1800141115

Sanchez-Azofeifa, A., Powers, J. S., Fernandes, G. W., & Quesada, M. (2013). *Tropical Dry Forests in the Americas: Ecology, Conservation, and Management*. CRC Press.

Scholander, P. F., Hammel, H. T., Bradstreet, E. D., & Hemmingsen, E. A. (1965). Sap pressure in vascular plants. *Science*, *148*(3668), 339–346.

Schwinning, S., & Ehleringer, J. R. (2001). Water use trade-offs and optimal adaptations to pulse-driven arid ecosystems. *Journal of Ecology*, *89*(3), 464–480. https://doi.org/10.1046/j.1365-2745.2001.00576.x

Simonin, K. A., Santiago, L. S., & Dawson, T. E. (2009). Fog interception by *Sequoia sempervirens* (D. Don) crowns decouples physiology from soil water deficit. *Plant, Cell & Environment*, *32*(7), 882–892. https://doi.org/10.1111/j.1365-3040.2009.01967.x

Stan, K., & Sanchez-Azofeifa, A. (2019). Tropical Dry Forest Diversity, Climatic Response, and Resilience in a Changing Climate. *Forests*, *10*(5), 443. https://doi.org/10.3390/f10050443

Tyree, M. T., & Sperry, J. S. (1989). Vulnerability of xylem to cavitation and embolism. *Annual Review of Plant Physiology and Plant Molecular Biology*, *40*(1), 19–36. https://doi.org/10.1146/annurev.pp.40.060189.000315

Vargas, A. I., Schaffer, B., Yuhong, L., & Sternberg, L. da S. L. (2017). Testing plant use

of mobile vs immobile soil water sources using stable isotope experiments. *New Phytologist*, *215*(2), 582–594. https://doi.org/10.1111/nph.14616

West, A. G., Patrickson, S. J., & Ehleringer, J. R. (2006). Water extraction times for plant and soil materials used in stable isotope analysis. *Rapid Communications in Mass Spectrometry*, *20*(8), 1317–1321. https://doi.org/10.1002/rcm.2456

White, J. W. C., Cook, E. R., Lawrence, J. R., & Wallace S., B. (1985). The DH ratios of sap in trees: Implications for water sources and tree ring DH ratios. *Geochimica et Cosmochimica Acta*, *49*(1), 237–246. https://doi.org/10.1016/0016-7037(85)90207-8

Wright, C., Kagawa-Viviani, A., Gerlein-Safdi, C., Mosquera, G. M., Poca, M., Tseng, H., & Chun, K. P. (2018). Advancing ecohydrology in the changing tropics: Perspectives from early career scientists. *Ecohydrology*, *11*(3), e1918. https://doi.org/10.1002/eco.1918

Zhao, L., Wang, L., Cernusak, L. A., Liu, X., Xiao, H., Zhou, M., & Zhang, S. (2016). Significant difference in hydrogen isotope composition between xylem and tissue water in *Populus euphratica*. *Plant, Cell & Environment*, *39*(8), 1848–1857. https://doi.org/10.1111/pce.12753

Zimmermann, U., Ehhalt, D., & Muennich, K. O. (1967). Soil-water movement and evapotranspiration: Changes in the isotopic composition of the water. *Pp 567-85 of Isotopes in Hydrology. Vienna, International Atomic Energy Agency, 1967.* https://www.osti.gov/biblio/4556792-soil-water-movement-evapotranspiration-changes-isotopic-composition-water

Zwieniecki, M. A., & Newton, M. (1996). Seasonal pattern of water depletion from soil rock profiles in a Mediterranean climate in southwestern Oregon. *Canadian Journal of Forest Research, 26*(8), 1346–1352. https://doi.org/10.1139/x26-150